DPNU-05-18
November, 2005

arXiv:hep-ph/0511312v2 16 Jan 2006

Dropping ρ and A_1 Meson Masses at Chiral Phase Transition in the Generalized Hidden Local Symmetry [*]

Masayasu Harada[1] and Chihiro Sasaki[2]

[1] *Department of Physics, Nagoya University, Nagoya, 464-8602, Japan*
[2] *Gesellschaft für Schwerionenforschung (GSI), 64291 Darmstadt, Germany*

We study the chiral symmetry restoration using the generalized hidden local symmetry (GHLS) which incorporates the rho and A_1 mesons as the gauge bosons of the GHLS and the pion as the Nambu-Goldstone boson consistently with the chiral symmetry of QCD. We show that a set of parameter relations, which ensures the first and second Weinberg sum rules, is invariant under the renormalization group evolution. Then, we found that the Weinberg sum rules together with the matching of the vector and axial-vector current correlators inevitably leads to *the dropping masses of both rho and A_1 mesons* at the symmetry restoration point, and that the mass ratio as well as the mixing angle between the pion and A_1 meson flows into one of three fixed points.

PACS numbers: 11.30.Rd, 12.28.Aw, 12.39.Fe

1. INTRODUCTION

Changes of the hadron masses are indications of the chiral symmetry restoration occurring in hot and/or dense QCD [1]. Dropping masses of hadrons following the Brown-Rho (BR) scaling [2] can be one of the most prominent candidates of the strong signal of the melting of the quark condensate $\langle\bar{q}q\rangle$ which is the order parameter of the spontaneous chiral symmetry breaking. Especially, the dropping of the ρ meson mass according to the BR scaling satisfactorily explained [3] the enhancement of di-electron mass spectra below the ρ/ω resonance observed at CERN SPS [4].

The vector manifestation (VM) [5] is the Wigner realization in which the ρ meson becomes massless degenerate with the pion at the chiral phase transition point. The VM is formulated in the effective field theory (EFT) based on the hidden local symmetry (HLS) [6, 7]. In the HLS theory we can perform the systematic chiral perturbation with the dynamical ρ meson included [8, 9, 10, 11]. Furthermore, the matching to QCD à la Wilson combined with the renormalization group equations (RGEs) gives several physical predictions in remarkable agreement with experiments [9, 12].

The formulation of the VM was done also in hot matter [13] and in dense matter [14], and a compelling evidence of dropping mass recently comes from the mass shift of the ω meson in nuclei measured by the KEK-PS E325 Experiment [15] and the CBELSA/TAPS Collaboration [16] and also from that of the ρ meson observed in the STAR experiment [17]. Since the VM formulated in the HLS theory provides a theoretical description of the dropping ρ mass which is protected by the existence of the fixed point (VM fixed point), we can study several other phenomena associated with the dropping ρ by expanding the HLS theory around the VM fixed point: Large violation of the vector dominance of the pion electromagnetic form factor should occur near the VM fixed point [18], which plays an important role [19] to explain the recent experimental data provided by NA60 [20]; The pion velocity near the restoration point is predicted as $v_\pi(T_c) = 0.83$-0.99 [21], which seems to be consistent with value extracted [22] from the recent data from the STAR collaboration at RHIC [23].

In the VM, it was assumed that the axial-vector and scalar mesons are decoupled from the theory near the phase transition point. However, the masses of these mesons may decrease following the BR scaling. Actually, recently in Ref. [24], it was proposed to extend the VM to include axial-vector mesons for explaining the anomalous ρ^0/π^- ratio measured in peripheral collisions by STAR [25]. There were several analyses with models including axial-vector mesons such as in Ref. [26]. These analyses are not based on the fixed point structure and found no significant reduction of the masses of axial-vector meson. Then, it is desirable to construct an EFT which includes the axial-vector meson as a dynamical degree of freedom, and study whether a fixed point structure exists and it can realize the light axial-vector meson.

There are several models which includes the axial-vector meson in addition to the pion and vector meson consistently with the chiral symmetry of QCD such as the "Massive Yang-Mills" field method [27], the anti-symmetric tensor field method [28] and the model based on the generalized hidden local symmetry (GHLS) [7, 29, 30, 31]. These models are equivalent [31, 32] at least tree-level on-shell amplitude is concerned. However, there are differences in the off-shell amplitude since the definitions of the off-shell fields are different in the models (see, e.g., Ref. [9]). Here we pick up the model based on the GHLS which is a natural extension of the HLS to include the axial-vector meson.

In this paper, we first develop the chiral perturbation theory (ChPT) with GHLS, in which a systematic low-energy expansion is possible even including the axial-vector meson in addition to the pseudoscalar and vector mesons as a dynamical degree of freedom. Then, we make the matching of the vector and axial-vector current correlators with those obtained by the operator product expansion (OPE) in the energy region higher than the axial-vector meson mass to find that the resultant set of the parameter relations satisfies the pole saturated forms of the first and second Weinberg sum rules. Based on the RGEs in the Wilsonian sense obtained in the ChPT with GHLS, the set of the parameter relations is shown to be stable against the renormalization group evolution.

---

[*] Main result of this work was presented in the talk "Systematic perturbation theory based on generalized hidden local symmetry" at Japan Physical Society meeting, March 24, 2005, Noda, Japan.

We further study the fate of the axial-vector meson near the chiral restoration point, and found that the Weinberg sum rules together with the matching necessarily leads to the dropping masses of both vector and axial-vector mesons. Interestingly, the ratio of masses of vector and axial-vector mesons as well as the mixing between the pseudoscalar and axial-vector mesons flows into one of three fixed points: They exhibit the VM–like, Ginzburg-Landau–like and Hybrid–like patterns of the chiral symmetry restoration.

This paper is organized as follows:

In section 2, we give a brief review on the GHLS. Construction of the ChPT with GHLS is done in section 3. In section 4, we make the matching to derive a set of parameter relations satisfying the pole saturated forms of the first and second Weinberg sum rules. This is shown to be stable against the renormalization group evolution. Section 5 is devoted to study the phase structure of the GHLS with the Weinberg sum rules kept satisfied. We show that both ρ and A_1 necessarily become massless at the phase transition point, and that the mass ratio flows into one of three fixed points. In section 6, we discuss the relation of three classes of the fixed point to the chiral representation mixing. Finally in section 7, we give a brief summary and discussions. We show the quantization of the GHLS theory based on the background field gauge in Appendix A, and several quantum corrections and RGEs in Appendix B.

2. GENERALIZED HIDDEN LOCAL SYMMETRY

The generalized hidden local symmetry (GHLS) is an extention of the hidden local symmetry (HLS), in which the axial-vector mesons as well as the vector mesons are introduced as the gauge bosons of the GHLS, in addition to the pseudoscalar mesons as the Nambu-Goldstone bosons associated with the spontaneous chiral symmetry breaking. In this section, we briefly review the GHLS following Refs. [7, 29, 30].

2.1. Lagrangian

The GHLS Lagrangian is based on the $G_{\rm global} \times G_{\rm local}$ symmetry, where $G_{\rm global} = [SU(N_f)_L \times SU(N_f)_R]_{\rm global}$ is the chiral symmetry and $G_{\rm local} = [SU(N_f)_L \times SU(N_f)_R]_{\rm local}$ is the GHLS. The whole symmetry $G_{\rm global} \times G_{\rm local}$ is spontaneously broken down to a flavor diagonal $SU(N_f)_V$. The basic quantities are the GHLS gauge bosons L_μ and R_μ and three matrix valued variables ξ_L, ξ_R and ξ_M which are introduced as

$$U = \xi_L^\dagger \xi_M \xi_R \,, \tag{2.1}$$

where $N_f \times N_f$ special-unitary matrix U is a basic ingredient of the chiral perturbation theory (ChPT) [33, 34]. The transformation property of U under the chiral symmetry is given by

$$U \to g_L U g_R^\dagger \,, \tag{2.2}$$

where g_L and g_R are the elements of the chiral symmetry, $g_{L,R} \in [SU(N_f)_{L,R}]_{\rm global}$. The variables ξs transform as

$$\begin{aligned} \xi_{L,R} &\to h_{L,R} \cdot \xi_{L,R} \cdot g_{L,R}^\dagger \,, \\ \xi_M &\to h_L \cdot \xi_M \cdot h_R^\dagger \,, \end{aligned} \tag{2.3}$$

with $h_{L,R} \in [SU(N_f)_{L,R}]_{\rm local}$. The GHLS gauge fields L_μ and R_μ transform as

$$\begin{aligned} L_\mu &\to i h_L \partial h_L^\dagger + h_L L_\mu h_L^\dagger \,, \\ R_\mu &\to i h_R \partial h_R^\dagger + h_R R_\mu h_R^\dagger \,. \end{aligned} \tag{2.4}$$

The covariant derivatives of $\xi_{L,R,M}$ are given by

$$\begin{aligned} D_\mu \xi_L &= \partial_\mu \xi_L - i L_\mu \xi_L + i \xi_L \mathcal{L}_\mu \,, \\ D_\mu \xi_R &= \partial_\mu \xi_R - i R_\mu \xi_R + i \xi_R \mathcal{R}_\mu \,, \\ D_\mu \xi_M &= \partial_\mu \xi_M - i L_\mu \xi_M + i \xi_M R_\mu \,, \end{aligned} \tag{2.5}$$

where $\mathcal{L}_\mu$ and $\mathcal{R}_\mu$ are the external gauge fields introduced by gauging $G_{\rm global}$ symmetry.

The fundamental objects are the Maurer-Cartan 1-forms defined by

$$\begin{aligned} \hat\alpha^\mu_{L,R} &= D^\mu \xi_{L,R} \cdot \xi_{L,R}^\dagger / i \,, \\ \hat\alpha^\mu_M &= D^\mu \xi_M \cdot \xi_M^\dagger / (2i) \,, \end{aligned} \tag{2.6}$$

which transform as

$$\begin{aligned} \hat\alpha^\mu_{L,R} &\to h_{L,R} \hat\alpha^\mu_{L,R} h_{L,R}^\dagger \,, \\ \hat\alpha^\mu_M &\to h_L \hat\alpha^\mu_M h_L^\dagger \,. \end{aligned} \tag{2.7}$$

There are four independent terms, with the lowest derivatives, invariant under $G_{\rm global} \times G_{\rm local}$:

$$\begin{aligned} \mathcal{L}_V &= F^2 {\rm tr}\big[\hat\alpha_{\parallel\mu} \hat\alpha_\parallel^\mu\big] \,, \\ \mathcal{L}_A &= F^2 {\rm tr}\big[\hat\alpha_{\perp\mu} \hat\alpha_\perp^\mu\big] \,, \\ \mathcal{L}_M &= F^2 {\rm tr}\big[\hat\alpha_{M\mu} \hat\alpha_M^\mu\big] \,, \\ \mathcal{L}_\pi &= F^2 {\rm tr}\big[\big(\hat\alpha_{\perp\mu} + \hat\alpha_{M\mu}\big)\big(\hat\alpha_\perp^\mu + \hat\alpha_M^\mu\big)\big] \,, \end{aligned} \tag{2.8}$$

where F is the parameter carrying the mass dimension 1 [#1] and $\hat{\alpha}_{\parallel,\perp}$ are defined as

$$\hat{\alpha}^{\mu}_{\parallel,\perp} = \left(\xi_M \hat{\alpha}^{\mu}_R \xi^{\dagger}_M \pm \hat{\alpha}^{\mu}_L\right)/2\,. \tag{2.9}$$

Another building block is the gauge field strength of the GHLS defined by

$$\begin{aligned} L_{\mu\nu} &= \partial_\mu L_\nu - \partial_\nu L_\mu - i\big[L_\mu, L_\nu\big]\,, \\ R_{\mu\nu} &= \partial_\mu R_\nu - \partial_\nu R_\mu - i\big[R_\mu, R_\nu\big]\,. \end{aligned} \tag{2.10}$$

From these field strengths, the kinetic term of the gauge bosons are given by

$$\mathcal{L}_{\rm kin}(L_\mu, R_\mu) = -\frac{1}{4g^2}{\rm tr}\big[L_{\mu\nu}L^{\mu\nu} + R_{\mu\nu}R^{\mu\nu}\big]\,, \tag{2.11}$$

with g being the gauge coupling constant of the GHLS. Note that the parity invariance requires that there is only one gauge coupling.

By combining the four terms in Eq. (2.8) together with the kinetic term of the gauge fields in Eq. (2.11), the GHLS Lagrangian is given by

$$\mathcal{L} = a\mathcal{L}_V + b\mathcal{L}_A + c\mathcal{L}_M + d\mathcal{L}_\pi + \mathcal{L}_{\rm kin}(L_\mu, R_\mu)\,, \tag{2.12}$$

where a, b, c and d are dimensionless parameters to be determined by the underlying QCD.

2.2. Particle Identification

The symmetry breaking pattern of the GHLS is given as

$$\begin{aligned} &[SU(N_f)_L \times SU(N_f)_R]_{\rm local} \\ &\quad \times [SU(N_f)_L \times SU(N_f)_R]_{\rm global} \\ &\qquad \to\ SU(N_f)_V\ , \end{aligned} \tag{2.13}$$

which generates $3 \times (N_f^2 - 1)$ massless Nambu-Goldstone (NG) bosons. $2 \times (N_f^2 - 1)$ of the NG bosons are absorbed into the gauge bosons of the GHLS to give masses through the Higgs mechanism. $(N_f^2 - 1)$ NG bosons remain as the massless particles, which we identify with the pseudoscalar mesons π (pion and its flavor partners). On the other hand, we identify the gauge bosons $V_\mu = (R_\mu + L_\mu)/2$ with the vector mesons denoted by ρ (ρ meson and its flavor partners) and $A_\mu = (R_\mu - L_\mu)/2$ with the axial-vector mesons denoted as A_1 (a_1 meson and its flavor partners).

In the following, we specify the π and would-be NG bosons absorbed into ρ and A_1 by parameterizing $\xi_{L,R,M}$ as

$$\begin{aligned} \xi_R &= e^{i(\phi_\sigma + \phi_\perp)}\,, \\ \xi_L &= e^{i(\phi_\sigma - \phi_\perp)}\,, \\ \xi_M &= e^{2i\phi_p}\,. \end{aligned} \tag{2.14}$$

Three 1-forms are expanded into

$$\begin{aligned} \hat{\alpha}^{\mu}_{\parallel} &= \partial^\mu \phi_\sigma - V^\mu + \mathcal{V}^\mu + \cdots\,, \\ \hat{\alpha}^{\mu}_{\perp} &= \partial^\mu \phi_\perp - A^\mu + \mathcal{A}^\mu + \cdots\,, \\ \hat{\alpha}^{\mu}_{M} &= \partial^\mu \phi_p + A^\mu + \cdots\,, \end{aligned} \tag{2.15}$$

where the vector and axial-vector external gauge fields $\mathcal{V}_\mu$ and $\mathcal{A}_\mu$ are defined as

$$\mathcal{V}_\mu = \frac{1}{2}\left(\mathcal{R}_\mu + \mathcal{L}_\mu\right)\ , \quad \mathcal{A}_\mu = \frac{1}{2}\left(\mathcal{R}_\mu - \mathcal{L}_\mu\right)\ . \tag{2.16}$$

The $a\mathcal{L}_V$ term in the Lagrangian is expressed as

$$a\mathcal{L}_V = F_\sigma^2\,{\rm tr}\left[\{\partial^\mu\phi_\sigma - V^\mu + \mathcal{V}^\mu\}^2\right] + \cdots\ , \tag{2.17}$$

where

$$F_\sigma^2 = aF^2\ . \tag{2.18}$$

Then, the would-be NG boson absorbed into the longitudinal component of the V_μ is identified as

$$\sigma = F_\sigma\,\phi_\sigma\,. \tag{2.19}$$

The remaining three terms, $b\mathcal{L}_A + c\mathcal{L}_M + d\mathcal{L}_\pi$, are expressed as

$$\begin{aligned} &b\mathcal{L}_A + c\mathcal{L}_M + d\mathcal{L}_\pi \\ &= (b+d)F^2\,{\rm tr}\big[(\partial_\mu\phi_\perp)^2\big] \\ &\quad + (c+d)F^2\,{\rm tr}\big[(\partial_\mu\phi_p)^2\big] + (b+c)F^2\,{\rm tr}\big[(A_\mu)^2\big] \\ &\quad - 2bF^2\,{\rm tr}\big[A_\mu\partial^\mu\phi_\perp\big] + 2cF^2\,{\rm tr}\big[A_\mu\partial^\mu\phi_p\big] \\ &\quad + 2dF^2\,{\rm tr}\big[\partial_\mu\phi_\perp\,\partial^\mu\phi_p\big] + \cdots\,. \end{aligned} \tag{2.20}$$

This can be further reduced into

$$\begin{aligned} &\big(b\mathcal{L}_A + c\mathcal{L}_M + d\mathcal{L}_\pi\big)_{\rm kin} \\ &= (b+c)F^2\,{\rm tr}\big[(A_\mu + \partial\phi_q)^2\big] \\ &\qquad + \Big(d + \frac{bc}{b+c}\Big)F^2\,{\rm tr}\big[(\partial\phi_\pi)^2\big]\,, \end{aligned} \tag{2.21}$$

where we define ϕ_π and ϕ_q as

$$\begin{aligned} \phi_\pi &= \phi_\perp + \phi_p\,, \\ \phi_q &= \frac{1}{(b+c)}\Big[c\,\phi_p - b\,\phi_\perp\Big]\,. \end{aligned} \tag{2.22}$$

The properly normalized fields are given by

$$\pi = F_\pi\,\phi_\pi\ , \quad q = F_q\,\phi_q\ , \tag{2.23}$$

[#1] In Ref. [7, 29, 30], each term has the pion decay constant F_π^2 as the coefficient by taking the proper normalization. In this paper, however, we introduce F just as a parameter which carries mass dimension 1. In the latter section, we will define F_π as the coupling strength to the broken current by dissolving the π-A_1 mixing.

where F_π is the π decay constant and F_q is the decay constant of the would-be NG boson q. They are defined as

$$\begin{aligned} F_\pi^2 &= (d + c\,\zeta)F^2 \,, \\ F_q^2 &= (b + c)F^2 \,, \end{aligned} \tag{2.24}$$

where

$$\zeta = \frac{b}{b+c} \,. \tag{2.25}$$

Let us introduce the ρ (ρ meson and its flavor partners) and A_1 (a_1 meson and its flavor partners) as

$$V^\mu = g\rho^\mu \,, \qquad A^\mu = gA_1^\mu \,. \tag{2.26}$$

Then, expanding the Lagrangian (2.12) in terms of the π, V_μ and A_μ fields taking the unitary gauge $\phi_q = \phi_\sigma = 0$ [#2], we find the following expressions for the masses of vector and axial-vector mesons M_{ρ,A_1}, the ρ-γ mixing strength g_ρ [#3] and strength of the coupling of the A_1 meson to the axial-vector current g_{A_1}:

$$\begin{aligned} M_\rho &= gF_\sigma \,, \qquad & M_{A_1} &= gF_q \,, \\ g_\rho &= gF_\sigma^2 \,, \qquad & g_{A_1} &= gbF^2 \,. \end{aligned} \tag{2.27}$$

3. CHIRAL PERTURBATION THEORY WITH THE GHLS

In this section, we construct the chiral perturbation theory (ChPT) based on the generalized hidden local symmetry (GHLS).

3.1. General Concept

In the HLS theory, thanks to the gauge invariance, it is possible to perform the derivative expansion systematically. In this ChPT with HLS (See, for a review, Ref. [9]), the vector meson mass is considered as small compared with the chiral symmetry breaking scale Λ_χ, by assigning $\mathcal{O}(p)$ to the HLS gauge coupling [10, 11]:

$$g \sim \mathcal{O}(p) \,. \tag{3.1}$$

We adopt the same order assignment for both ρ and A_1 mesons in the GHLS, i.e., $m_\rho \sim m_{A_1} \sim \mathcal{O}(p)$. Using the above counting rule, we can systematically incorporate the quantum corrections to several physical quantities.

In the following, we examine the smallness of our expansion parameter $m_{\rho,A_1}/\Lambda_\chi$. Similarly to the smallness of m_ρ/Λ_χ discussed in Ref. [9], the smallness of the expansion parameters $m_{\rho,A_1}/\Lambda_\chi \ll 1$ can be justified in a large number of colors N_c of QCD as follows: In the large N_c limit, the pion decay constant F_π scales as $\sqrt{N_c}$ which implies that Λ_χ scales as $\Lambda_\chi \sim 4\pi F_\pi \sim \sqrt{N_c}$. On the other hand, the masses of vector and axial-vector mesons, m_{ρ,A_1}, do not scale with N_c. So the ratios $m^2_{\rho,A_1}/F_\pi^2$ scales as $1/N_c$, and becomes small in the large N_c QCD:

$$\frac{m^2_{\rho,A_1}}{\Lambda_\chi^2} = \frac{m^2_{\rho,A_1}}{(4\pi F_\pi)^2} \sim \frac{1}{N_c} \ll 1 . \tag{3.2}$$

Thus we can perform the derivative expansion in the large N_c limit, and extrapolate the results to the real-life QCD with $N_c = 3$.

3.2. One-loop Calculations

Let us calculate the quantum corrections from the π, ρ and A_1 meson loops to five leading-order parameters of the GHLS Lagrangian. We make the quantization using the background field gauge in 't Hooft-Feynman gauge, which is summarized in Appendix A.

We would like to stress that it is important to include the quadratic divergences to obtain the RGEs in the Wilsonian sense. In this paper, following Refs. [9, 12, 35], we adopt the dimensional regularization and identify the quadratic divergences with the presence of poles of ultraviolet origin at $n = 2$ [36]. This can be done by the following replacement in the Feynman integrals:

$$\begin{aligned} \int \frac{d^nk}{i(2\pi)^n}\frac{1}{-k^2} &\to \frac{\Lambda^2}{(4\pi)^2} \,, \\ \int \frac{d^nk}{i(2\pi)^n}\frac{k_\mu k_\nu}{[-k^2]^2} &\to -\frac{\Lambda^2}{2(4\pi)^2}g_{\mu\nu} \,. \end{aligned} \tag{3.3}$$

On the other hand, the logarithmic divergence is identified with the pole at $n = 4$:

$$\frac{1}{\bar\epsilon} + 1 \to \ln\Lambda^2 \,, \tag{3.4}$$

[#2] When the gauge is fixed by taking $\xi_M = 1$ and $\xi_R = \xi_L^\dagger = e^{i\pi/F_\pi}$, the A_1-π mixing is dissolved afterwards, as shown in Refs. [7, 29, 30]. In this paper, on the other hand, we introduced π field to eliminate the A_1-π mixing, and fixed the gauge to the unitary gauge by taking

$$\begin{aligned} \xi_M &= \exp\left[2i\,\zeta\,\phi_\pi\right] \,, \\ \xi_R = \xi_L &= \exp\left[i(1-\zeta)\phi_\pi\right] \,. \end{aligned}$$

As emphasized in Refs. [7, 29] the above parameterization is converted into $\xi_M = 1$ and $\xi_R = \xi_L^\dagger = e^{i\pi/F_\pi}$ by the "gauge transformation":

$$g_R = g_L^\dagger = \exp\left[i\,\zeta\,\phi_\pi\right] \,,$$

as

$$\begin{aligned} \xi'_M &= g_L\,\xi_M\,g_R^\dagger = 1 \,, \\ \xi'_R &= g_R\,\xi_R = e^{i\phi_\pi} \,, \\ \xi'_L &= g_L\,\xi_L = e^{-i\phi_\pi} \,. \end{aligned}$$

[#3] The photon field A_μ for $N_f = 3$ is embedded into $\mathcal{V}_\mu$ as

$$\mathcal{V}_\mu = eA_\mu Q, \quad Q = \begin{pmatrix} 2/3 & & \\ & -1/3 & \\ & & -1/3 \end{pmatrix} ,$$

with e being the coupling of the external gauge bosons.

where

$$\frac{1}{\bar{\epsilon}} \equiv \frac{2}{4-n} - \gamma_E + \ln(4\pi)\,, \tag{3.5}$$

with γ_E being the Euler constant.

In the following, we consider the two-point functions of $\bar{V}^\mu$-$\bar{V}^\nu$, $\bar{A}^\mu$-$\bar{A}^\nu$, $\bar{\mathcal{A}}_\perp^\mu$-$\bar{A}^\nu$ and $\bar{\mathcal{A}}_M^\mu$-$\bar{\mathcal{A}}_\perp^\nu$ (see Appendix A for definitions of the background fields), which we express as $\Pi^{\mu\nu}_{\bar{V}\bar{V}}$, $\Pi^{\mu\nu}_{\bar{A}\bar{A}}$, $\Pi^{\mu\nu}_{\bar{\mathcal{A}}_\perp\bar{A}}$, $\Pi^{\mu\nu}_{\bar{\mathcal{A}}_M\bar{\mathcal{A}}_\perp}$, respectively. We divide each of these two-point functions into two parts as

$$\Pi^{\mu\nu}(p) = \Pi^S(p^2) g^{\mu\nu} + \Pi^{LT}(p^2)(p^2 g^{\mu\nu} - p^\mu p^\nu)\,. \tag{3.6}$$

At the bare level, the relevant parts are expressed as

$$\begin{aligned}
\Pi^{(\text{bare})S}_{\bar{V}\bar{V}} &= a_{\text{bare}} F^2\,,\\
\Pi^{(\text{bare})LT}_{\bar{V}\bar{V}} &= -\frac{1}{g^2_{\text{bare}}} + 2 z^{LR}_{\text{bare}}\,,\\
\Pi^{(\text{bare})S}_{\bar{A}\bar{A}} &= (b_{\text{bare}} + c_{\text{bare}}) F^2\,,\\
\Pi^{(\text{bare})LT}_{\bar{A}\bar{A}} &= -\frac{1}{g^2_{\text{bare}}} - 2 z^{LR}_{\text{bare}}\,,\\
\Pi^{(\text{bare})S}_{\bar{\mathcal{A}}_\perp\bar{A}} &= -b_{\text{bare}} F^2\,,\\
\Pi^{(\text{bare})S}_{\bar{\mathcal{A}}_M\bar{\mathcal{A}}_\perp} &= d_{\text{bare}} F^2\,,
\end{aligned} \tag{3.7}$$

where z^{LR}_{bare} is the coefficient of $\mathcal{O}(p^4)$ terms which proportional to $\text{tr}\left[L_{\mu\nu}\xi_M R^{\mu\nu}\xi_M^\dagger\right]$ [#4].

In Appendix B, we list the diagrams contributing to $\Pi^{\mu\nu}$ at one-loop level and the quantum corrections from those diagrams (see Figs. 4-7 and Eqs. (B.3)-(B.6)). From Eq. (3.7), we find that the divergences proportional to $g^{\mu\nu}$ in the two-point functions are renormalized by $a_{\text{bare}}, b_{\text{bare}}, c_{\text{bare}}$ and d_{bare} and those proportional to $(p^2 g^{\mu\nu} - p^\mu p^\nu)$ are renormalized by g_{bare} and z^{LR}_{bare}. Thus we require the following renormalization conditions:

$$\begin{aligned}
& a_{\text{bare}} F^2 + \Pi^S_{\bar{V}\bar{V}}\big|_{\text{div}} = (\text{finite})\,,\\
& -b_{\text{bare}} F^2 + \Pi^S_{\bar{\mathcal{A}}_\perp\bar{A}}\big|_{\text{div}} = (\text{finite})\,,\\
& c_{\text{bare}} F^2 + \Pi^S_{\bar{A}\bar{A}}\big|_{\text{div}} + \Pi^S_{\bar{\mathcal{A}}_\perp\bar{A}}\big|_{\text{div}} = (\text{finite})\,,\\
& d_{\text{bare}} F^2 + \Pi^S_{\bar{\mathcal{A}}_M\bar{\mathcal{A}}_\perp}\big|_{\text{div}} = (\text{finite})\,,\\
& -\frac{1}{g^2_{\text{bare}}} + \frac{1}{2}\left[\Pi^{LT}_{\bar{V}\bar{V}}\big|_{\text{div}} + \Pi^{LT}_{\bar{A}\bar{A}}\big|_{\text{div}}\right] = (\text{finite})\,.
\end{aligned} \tag{3.8}$$

From the above renormalization conditions, we obtain the renormalization group equations (RGEs) for the parameters a, b, c, d and the GHLS gauge coupling g, which are listed in Eqs. (B.7)-(B.11).

4. WEINBERG'S SUM RULES

Let us start with the axial-vector and vector current correlators defined by

$$\begin{aligned}
& G_A(Q^2)(q^\mu q^\nu - q^2 g^{\mu\nu})\delta_{ab}\\
&\qquad = \int d^4x\, e^{iqx} \left\langle 0\right| T\, J^\mu_{5a}(x) J^\nu_{5b}(0) \left|0\right\rangle\,,\\
& G_V(Q^2)(q^\mu q^\nu - q^2 g^{\mu\nu})\delta_{ab}\\
&\qquad = \int d^4x\, e^{iqx} \left\langle 0\right| T\, J^\mu_{a}(x) J^\nu_{b}(0) \left|0\right\rangle\,,
\end{aligned} \tag{4.1}$$

where $Q^2 = -q^2$ is the space-like momentum, J^μ_{5a} and J^μ_a are the axial-vector and vector currents and $(a,b) = 1,\ldots,N_f^2 - 1$ denotes the flavor index. At the leading order of the GHLS the current correlators $G_{A,V}$ are expressed as

$$\begin{aligned}
G_A(Q^2) &= \frac{F_\pi^2}{Q^2} + \frac{F_{A_1}^2}{M_{A_1}^2 + Q^2}\,,\\
G_V(Q^2) &= \frac{F_\rho^2}{M_\rho^2 + Q^2}\,,
\end{aligned} \tag{4.2}$$

where the A_1 and ρ decay constants are defined by

$$\begin{aligned}
F_{A_1}^2 &= \left(\frac{g_{A_1}}{M_{A_1}}\right)^2 = \frac{b^2}{b+c} F^2\,,\\
F_\rho^2 &= \left(\frac{g_\rho}{M_\rho}\right)^2 = a F^2\,.
\end{aligned} \tag{4.3}$$

The same correlators are evaluated by the OPE as [38]

$$\begin{aligned}
G_A^{(\text{OPE})}(Q^2) &= \frac{1}{8\pi^2}\left[-\left(1 + \frac{\alpha_s}{\pi}\right)\ln\frac{Q^2}{\mu^2}\right.\\
&\quad \left. + \frac{\pi^2}{3}\frac{\left\langle \frac{\alpha_s}{\pi} G_{\mu\nu}G^{\mu\nu}\right\rangle}{Q^4} + \frac{\pi^3}{3}\frac{1408}{27}\frac{\alpha_s \left\langle \bar{q}q\right\rangle^2}{Q^6}\right]\,,\\
G_V^{(\text{OPE})}(Q^2) &= \frac{1}{8\pi^2}\left[-\left(1 + \frac{\alpha_s}{\pi}\right)\ln\frac{Q^2}{\mu^2}\right.\\
&\quad \left. + \frac{\pi^2}{3}\frac{\left\langle \frac{\alpha_s}{\pi} G_{\mu\nu}G^{\mu\nu}\right\rangle}{Q^4} - \frac{\pi^3}{3}\frac{896}{27}\frac{\alpha_s \left\langle \bar{q}q\right\rangle^2}{Q^6}\right]\,,
\end{aligned} \tag{4.4}$$

where μ is the renormalization scale of QCD. An important result obtained from the above forms is that the difference between two correlators scales as $1/Q^6$:

$$G_A^{(\text{OPE})}(Q^2) - G_V^{(\text{OPE})}(Q^2) = \frac{32\pi}{9}\frac{\alpha_s \left\langle \bar{q}q\right\rangle^2}{Q^6}\,. \tag{4.5}$$

Since the above forms of the correlators in the OPE are valid in the high energy region, we consider the difference of the correlators in the GHLS in the energy region higher than the A_1 meson mass, i.e., $Q^2 \gg M_A^2$. In the high energy region, two correlators in the GHLS given in

---

[#4] Some of the possible $\mathcal{O}(p^4)$ terms contributing to three- and four-point functions are listed in Refs. [7, 37]. A complete list of the anomalous terms at $\mathcal{O}(p^4)$ is given in Ref. [31].

Eq. (4.2) are expanded as

$$G_A(Q^2) = \frac{F_\pi^2 + F_{A_1}^2}{Q^2} - \frac{F_{A_1}^2 M_{A_1}^2}{Q^4} + \frac{F_{A_1}^2 M_{A_1}^4}{Q^6} \,,$$
$$G_A(Q^2) = \frac{F_\rho^2}{Q^2} - \frac{F_\rho^2 M_\rho^2}{Q^4} + \frac{F_\rho^2 M_\rho^4}{Q^6} \,. \qquad (4.6)$$

From the above expressions, the difference of two correlators is given by

$$G_A(Q^2) - G_V(Q^2) = \frac{F_\pi^2 + F_{A_1}^2 - F_\rho^2}{Q^2} + \frac{F_{A_1}^2 M_{A_1}^2 - F_\rho^2 M_\rho^2}{Q^4} + \frac{F_{A_1}^2 M_{A_1}^4 - F_\rho^2 M_\rho^4}{Q^6} \,. \qquad (4.7)$$

We require that the high energy behavior of the difference between two correlators in the GHLS agrees with that in the OPE: $G_A(Q^2) - G_V(Q^2)$ in the GHLS scales as $1/Q^6$. This requirement can be satisfied only if the following relations are satisfied:

$$F_\pi^2 + F_{A_1}^2 = F_\rho^2 \,,$$
$$F_{A_1}^2 M_{A_1}^2 = F_\rho^2 M_\rho^2 \,, \qquad (4.8)$$

which are nothing but the pole saturated forms of the Weinberg first and second sum rules [39]. In terms of the parameters of the GHLS Lagrangian, the above relations can be satisfied if we take

$$a = b \,, \quad d = 0 \,. \qquad (4.9)$$

Now, let us study whether the above relations in Eq. (4.9) are stable against the quantum corrections. Taking $a = b$ and $d = 0$ in the RGEs for a, b and d shown in Eqs. (B.8), (B.9) and (B.10), we obtain

$$\mu \frac{d(aF^2)}{d\mu} = \frac{N_f}{(4\pi)^2}\left[\mu^2 + 3ag^2F^2\right] , \qquad (4.10)$$
$$\mu \frac{d(bF^2)}{d\mu} = \frac{N_f}{(4\pi)^2}\left[\mu^2 + 3ag^2F^2\right] , \qquad (4.11)$$
$$\mu \frac{d(dF^2)}{d\mu} = 0 \,. \qquad (4.12)$$

The first two RGEs lead to

$$\mu \frac{d(a-b)}{d\mu} = 0 \,. \qquad (4.13)$$

The RGEs in Eqs. (4.12) and (4.13) imply that the parameter relations $a = b$ and $d = 0$ are stable against the renormalization group evolution, i.e., *the non-renormalization of the Weinberg sum rules expressed in terms of the leading order parameters in the GHLS.*

At the last of this section, we look into a set of the parameter relations in Eq. (4.9) to the symmetry structure of the GHLS theory. When we take $a = b$ and $d = 0$, the GHLS Lagrangian given in Eq. (2.8) is rewritten as

$$a\mathcal{L}_V + b\mathcal{L}_A + c\mathcal{L}_M + d\mathcal{L}_\pi = -8aF^2 \,\mathrm{tr}\left[\left(D_\mu \xi_R\right)^2 + \left(D_\mu \xi_L\right)^2\right] - 4cF^2 \,\mathrm{tr}\left[\left(D_\mu \xi_M\right)^2\right] \,. \qquad (4.14)$$

When we further switch off the gauge coupling, the symmetry of the Lagrangian becomes enhanced as $G_{\text{global}} \times [G_{\text{global}}]^2 = [G_{\text{global}}]^3 = [SU(N_f)_L \times SU(N_f)_R]^3$. This implies that three variables ξ_L, ξ_R and ξ_M couple to each other only through the GHLS gauge bosons V_μ and A_μ, when the gauge coupling is switched on. This structure is generally refereed as the "theory space locality" [40, 41, 42, 43]. From the above consideration, we see that, in the GHLS, the requirement of the Weinberg sum rules automatically leads to the "theory space locality" [44]. In general cases, the "theory space locality" is satisfied only at tree level, since the enhanced symmetry is broken when the gauge coupling is switched on. However, our result of the stability of the relations $a = b$ and $d = 0$ implies that *the "theory space locality" in the leading order Lagrangian is stable against the quantum correction* at least at one-loop level.

5. CHIRAL SYMMETRY RESTORATION

In this section, we study the chiral phase transition keeping the first and second Weinberg sum rules in the GHLS.

Equations (4.5) and (4.7) with the Weinberg sum rules (4.8) give the following matching condition in the high-energy region:

$$F_{A_1}^2 M_{A_1}^4 - F_\rho^2 M_\rho^4 = F_\rho^2 M_\rho^2 \left(M_{A_1}^2 - M_\rho^2\right) = \frac{32\pi\alpha_s}{9} \langle \bar{q}q \rangle^2 \,, \qquad (5.1)$$

which is a measure of the spontaneous chiral symmetry breaking. In terms of the parameters of the GHLS Lagrangian this is expressed as

$$a^2 \cdot c \cdot g^4 \propto \langle \bar{q}q \rangle^2 \,. \qquad (5.2)$$

When the chiral restoration point is approached, the quark condensate approaches zero:

$$\langle \bar{q}q \rangle \;\rightarrow\; 0 \,, \qquad (5.3)$$

This implies that the condition

$$a^2 \cdot c \cdot g^4 \;\rightarrow\; 0 \qquad (5.4)$$

is satisfied when the chiral symmetry is restored. From this condition we see that at least one parameter among a, c and g must go to zero at the chiral symmetry restoration point.

Let us first consider the possibility that the parameter a goes to zero at a high energy scale, say Λ: $a(\Lambda) \to 0$. The RGE for a given in Eq. (4.10) implies that $a = 0$ is not a fixed point, and thus one cannot achieve the equality of the axial-vector and vector current correlator in the energy region below Λ which is required by the chiral symmetry restoration. To make the matters worse, the RGE for a leads to $a(\mu) < 0$ for $\mu < \Lambda$, and $M_\rho^2 < 0$, which is of course unacceptable. From these, we cannot take $a \to 0$.

We next consider the possibility of $c(\Lambda) \to 0$. From Eq. (B.9), the RGE for c in the case of $a = b$ and $d = 0$ is obtained as

$$\mu \frac{d(cF^2)}{d\mu} = \frac{N_f}{(4\pi)^2}\left[2\mu^2 + 6cg^2F^2\right] . \tag{5.5}$$

We can easily see that $c = 0$ is not a fixed point, which implies that the equality of two current correlators cannot be satisfied in the energy region below Λ even if we equate them at Λ. Furthermore, negative c leads to $M_\rho^2/M_{A_1}^2 = a/(a+c) > 1$, which is unacceptable, either. Thus $c \to 0$ cannot be achieved at the restoration point.

Finally, we study the possibility of $g \to 0$. From Eq. (B.11), the RGE for g with $a = b$ and $d = 0$ is reduced to

$$\mu \frac{dg^2}{d\mu} = -\frac{N_f}{(4\pi)^2}\frac{43}{3}g^4 , \tag{5.6}$$

which certainly has the fixed point at $g = g^* = 0$. Then, the symmetry restoration in the GHLS can be realized only if the following condition is met:

$$g \ \to \ g^* = 0 . \tag{5.7}$$

This condition implies the massless ρ and A_1 mesons, since both masses are proportional to the gauge coupling g. [#5] Thus we conclude that, *when we require the first and second Weinberg sum rules to be satisfied, the chiral symmetry restoration in the GHLS required through the matching to QCD can be realized with masses of ρ and A_1 mesons vanishing at the restoration point*:

$$M_\rho \ \to \ 0 , \quad M_{A_1} \ \to \ 0 . \tag{5.8}$$

We next consider the fate of two parameters a $(= b)$ and c. As we can see easily from Eq. (5.1) or Eq. (5.2), matching of the GHLS to QCD does not provide any conditions for a and c other than $g \to 0$ at the restoration point. For $a = b$ and $d = 0$ the definitions of the parameter ζ and the pion decay constant given in Eqs. (2.24) and (2.25) are rewritten as

$$F_\pi^2 \ = \ \frac{ac}{a+c}F^2 , \tag{5.9}$$

$$\zeta \ = \ \frac{a}{a+c} = \frac{M_\rho^2}{M_{A_1}^2} , \tag{5.10}$$

From this, we see that the parameter ζ plays an important role, which controls the fate of the ratio of ρ and A_1 meson masses at the symmetry restoration. Below, we shall investigate the phase structure of the GHLS to see how the mass ratio ζ is determined at the symmetry restoration point and characterizes the possible patterns of chiral symmetry restoration governed by several fixed points.

To study the phase structure of the GHLS through the RGEs for a, c and g, it is convenient to introduce the following dimensionless parameters associated with a, c and g:

$$\begin{aligned} X(\mu) &= \frac{N_f}{2(4\pi)^2}\frac{\mu^2}{a(\mu)F^2} , \\ Y(\mu) &= \frac{N_f}{2(4\pi)^2}\frac{\mu^2}{c(\mu)F^2} , \\ G(\mu) &= \frac{N_f}{2(4\pi)^2}g^2(\mu) . \end{aligned} \tag{5.11}$$

In terms of X and Y, the order parameter F_π and the mass ratio ζ are expressed as

$$W(\mu) = \frac{N_f}{2(4\pi)^2}\frac{\mu^2}{F_\pi^2(\mu)} = X(\mu) + Y(\mu) , \tag{5.12}$$

$$\zeta(\mu) = \frac{Y(\mu)}{X(\mu)+Y(\mu)} . \tag{5.13}$$

The RGEs shown in Eqs. (4.10), (5.5) and (5.6) are rewritten as

$$\begin{aligned} \mu\frac{dX}{d\mu} &= 2X(1 - X - 3G) , \\ \mu\frac{dY}{d\mu} &= 2Y(1 - 2Y - 6G) , \\ \mu\frac{dG}{d\mu} &= -\frac{86}{3}G^2 . \end{aligned} \tag{5.14}$$

From these RGEs we find that three non-trivial fixed points and one trivial fixed point. The trivial fixed point is given by

$$(X^*, Y^*, G^*) = (0, 0, 0) , \tag{5.15}$$

while non-trivial ones are

$$\begin{aligned} \text{A}: \quad & (X^*, Y^*, G^*) = (1, 0, 0) , \\ \text{B}: \quad & (X^*, Y^*, G^*) = (0, 1/2, 0) , \\ \text{C}: \quad & (X^*, Y^*, G^*) = (1, 1/2, 0) . \end{aligned} \tag{5.16}$$

[#5] This symmetry restoration is similar to the vector manifestation (VM) [5, 9], in which the massless ρ becomes the chiral partner of the pion. As is stressed for the VM in Ref. [9], the symmetry restoration here should also be considered only as a limit with bare parameters approaching the fixed point: An enhancement of the global symmetry occurs when we take $g = 0$ from the beginning. While for non-zero gauge coupling, even if it is very tiny, the global symmetry in the GHLS is only the chiral symmetry consistently with QCD.

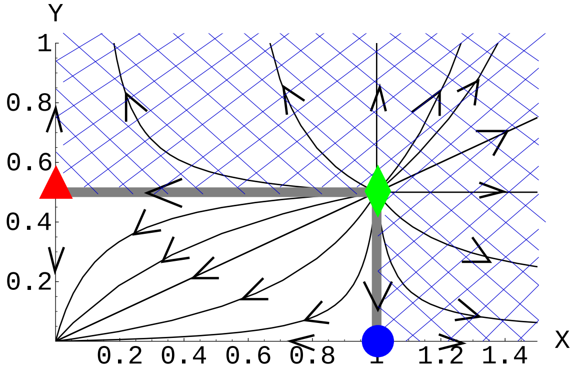

FIG. 1: Phase diagram on $G = 0$ plane. Arrows on the flows are written from the ultraviolet to the infrared. Gray lines divide the broken phase (inside) and the symmetric phase (outside; cross-hatched area). Points denoted by ▲, ● and ♦ express the fixed point $(X, Y) = (0, 1/2)$, $(1, 0)$ and $(1, 1/2)$ respectively.

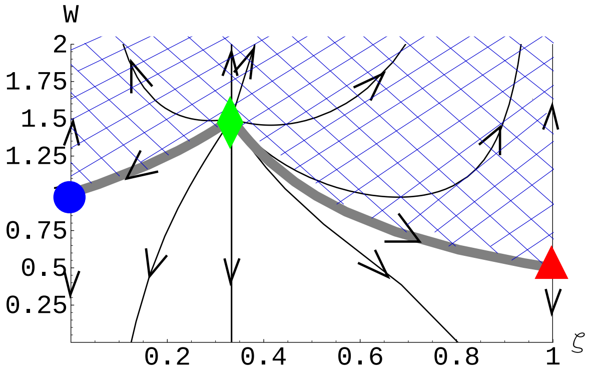

FIG. 2: Phase diagram on ζ-W plane. Arrows on the flows are written from the ultraviolet to the infrared. Gray lines divide the broken phase (lower side) and the symmetric phase (upper side; cross-hatched area). Points denoted by ▲, ● and ♦ express the fixed point $(\zeta, W) = (1, 1/2)$, $(0, 1)$ and $(1/3, 3/2)$ respectively.

As we concluded above, the symmetry restoration can be realized only if we have $G \to 0$ at the restoration point. Since $G = 0$ is the only fixed point of the RGE for G, we concentrate on the case with $G = 0$. In such a case, the RGE flows are confined on the X-Y plane. Furthermore, since both ρ and A_1 mesons are massless, we can use the RGEs for X and Y all the way down to the low-energy limit, $\mu = 0$. Then, the phase of the GHLS is determined by the on-shell pion decay constant $F_\pi(\mu = 0)$, or equivalently W defined in Eq. (5.12), as

$$\begin{aligned} &W(\mu = 0) = 0 \qquad \text{broken phase} \\ &W(\mu = 0) \neq 0 \qquad \text{symmetric phase} \end{aligned} \tag{5.17}$$

We show the flow diagram in X-Y plane in Fig. 1. The phase boundary is specified by $F_\pi(0) = 0$ which is realized at each fixed point listed in Eq. (5.16). The fixed point A implies $a(0) = 0$ and $c(0) \neq 0$, B entails $a(0) \neq 0$ and $c(0) = 0$, and C gives us $a(0) = c(0) = 0$. We note that $a(0) = 0$ and/or $c(0) = 0$ are realized due to the quadratic running of the RGEs although the bare parameters a_{bare} and c_{bare} are non-zero even at the restoration point.

In order to clarify the implication of each fixed point, we map the phase diagram in the X-Y plane onto the ζ-W plane, which is shown in Fig. 2. Three fixed points (5.16) are turned into

$$\begin{aligned} \text{A}: &\quad (\zeta^*, W^*) = (1, 1/2)\,, \\ \text{B}: &\quad (\zeta^*, W^*) = (0, 1)\,, \\ \text{C}: &\quad (\zeta^*, W^*) = (1/3, 3/2)\,. \end{aligned} \tag{5.18}$$

From this we can distinguish three patterns of the chiral symmetry restoration characterized by three fixed points by the values of the ratio of ρ and A_1 meson masses expressed by ζ as in Eq. (5.10) as follows: At the fixed point A, ζ goes to 1, which implies that the ρ meson mass degenerates into the A_1 meson mass. We shall call this restoration pattern the Ginzburg-Landau (GL) type. At the fixed point B, on the other hand, the ρ meson becomes massless faster than the A_1 meson since ζ goes to zero. This can be called the vector manifestation (VM) type. The fixed point C is the ultraviolet fixed point in any direction, so that it is not so stable as to A and B. Nevertheless, if it is chosen, the mass ratio approaches to 1/3 which we shall call the hybrid type.

To summarize, we find that the chiral symmetry restoration in the GHLS required through the matching to QCD can be realized only if the masses of ρ and A_1 mesons vanish at the restoration point:

$$M_\rho \to 0\,, \quad M_{A_1} \to 0\,, \tag{5.19}$$

and that the ratio of these masses flows into one of the following three fixed points:

$$\begin{aligned} \text{GL-type} &: M_\rho^2/M_{A_1}^2 \to 1\,, \\ \text{VM-type} &: M_\rho^2/M_{A_1}^2 \to 0\,, \\ \text{Hybrid-type} &: M_\rho^2/M_{A_1}^2 \to 1/3\,. \end{aligned} \tag{5.20}$$

6. CHIRAL REPRESENTATION MIXING

In this section, we discuss the relation of three classes of the fixed point studied in previous section to the chiral representation mixing.

In the broken phase of the chiral symmetry, the eigenstates of the chiral representation under $SU(N_f)_L \times SU(N_f)_R$ do not generally agree with the mass eigenstates due to the existence of the Nambu-Goldstone bosons, i.e., there exists a representation mixing. By extending the analysis done in Ref. [45, 46] for two-flavor QCD, the scalar, pseudoscalar, longitudinal vector and axial-vector mesons belong to the following representations:

$$\begin{aligned}|s\rangle &= |(N_f, N_f^*) \oplus (N_f^*, N_f)\rangle\,,\\ |\pi\rangle &= |(N_f, N_f^*) \oplus (N_f^*, N_f)\rangle \sin\psi\\ &\quad + |(1, N_f^2-1) \oplus (N_f^2-1, 1)\rangle \cos\psi\,,\\ |\rho\rangle &= |(1, N_f^2-1) \oplus (N_f^2-1, 1)\rangle\,,\\ |A_1\rangle &= |(N_f, N_f^*) \oplus (N_f^*, N_f)\rangle \cos\psi\\ &\quad - |(1, N_f^2-1) \oplus (N_f^2-1, 1)\rangle \sin\psi\,, \end{aligned} \tag{6.1}$$

where ψ denotes the mixing angle. The value of ψ for $N_f = 2$ is estimated as about $\psi \simeq 45\,°$.

It can be expected that the above representation mixing is dissolved when the chiral symmetry is restored. From Eq. (6.1), one can easily see that there are two possibilities for pattern of chiral symmetry restoration. One possible pattern is the case where $\cos\psi \to 0$ when we approach the critical point. In this case, the pion belongs to $|(N_f, N_f^*) \oplus (N_f^*, N_f)\rangle$ and becomes the chiral partner of the scalar meson. The longitudinal vector and axial-vector mesons are in the same multiplet $|(1, N_f^2-1) \oplus (N_f^2-1, 1)\rangle$. This is the standard Ginzburg-Landau (GL) scenario of the chiral symmetry restoration. Another possibility is the case where $\sin\psi \to 0$ when we approach the critical point. In this case, the pion belongs to pure $|(1, N_f^2-1) \oplus (N_f^2-1, 1)\rangle$ and its chiral partner is now the (longitudinal) vector meson. The scalar meson joins with the longitudinal part of the axial-vector meson in the same representation $|(N_f, N_f^*) \oplus (N_f^*, N_f)\rangle$. This is the vector manifestation (VM) of chiral symmetry [5, 9].

Now we consider how the chiral representation mixing is expressed in the GHLS theory. When we take $d = 0$ in the Lagrangian, there are no $\phi_\perp$-ϕ_p mixing terms [see Eq. (2.21)]. Then we take the normalizations of $\phi_\perp$ and ϕ_p fields as follows:

$$\phi_\perp = \pi_\perp/\sqrt{bF^2}\,, \qquad \phi_p = p/\sqrt{cF^2}\,. \tag{6.2}$$

Since $\pi_\perp$ is included in ξ_L and ξ_R and p is in ξ_M, we identify $\pi_\perp$ with the field belonging to the chiral representation $(1, N_f^2-1) \oplus (N_f^2-1, 1)$ and p with $(N_f, N_f^*) \oplus (N_f^*, N_f)$ according to the transformation properties of ξ_L, ξ_R and ξ_M. Using Eqs. (2.22) and (2.24), we rewrite π and q in terms of $\pi_\perp$ and p as

$$\begin{aligned}\pi &= \sqrt{\zeta}\,p + \sqrt{1-\zeta}\,\pi_\perp\,,\\ q &= \sqrt{1-\zeta}\,p - \sqrt{\zeta}\,\pi_\perp\,.\end{aligned} \tag{6.3}$$

We compare the above expression to Eq. (6.1) and obtain that the chiral representation mixing angle is related to the mass ratio ζ as

$$\cos\psi = \sqrt{1-\zeta}\,, \qquad \sin\psi = \sqrt{\zeta}\,. \tag{6.4}$$

Then, from three fixed points (5.18) of the GHLS at the symmetry restoration point, the fate of the chiral representation mixing is determined as follows:

$$\begin{aligned}&\text{GL-type} \ :\ \cos\psi \ \to\ 0\,,\\ &\text{VM-type} \ :\ \sin\psi \ \to\ 0\,,\\ &\text{Hybrid-type} \ :\\ &\qquad \sin\psi \ \to\ \sqrt{\frac{1}{3}}\,, \quad \cos\psi \ \to\ \sqrt{\frac{2}{3}}\,.\end{aligned} \tag{6.5}$$

7. SUMMARY AND DISCUSSIONS

In this paper, we developed the chiral perturbation theory (ChPT) with the generalized hidden local symmetry (GHLS) as an effective field theory (EFT) of QCD for pions, vector and axial-vector mesons. We showed that the first and second Weinberg sum rules expressed in terms of the leading order parameters, which is required by the equality of the high-energy behaviors of the current correlators of the GHLS to the ones in QCD, can be satisfied by a special parameter choice, $a = b$ and $d = 0$, corresponding to the theory space locality. Our analysis using the one-loop RGEs provides that this parameter choice is stable against the RG evolution, i.e., the non-renormalization of the Weinberg sum rules in the GHLS: The completion of the sum rules at the bare level is kept even at quantum level.

With the set of parameters corresponding to the Weinberg sum rules, we investigated the phase structure of the GHLS theory. We found that both ρ and A_1 meson become massless at the chiral phase transition point, which is protected by the fact that the GHLS gauge coupling constant g goes to zero as the only fixed point of the RGE for g:

$$M_\rho \ \to\ 0\,, \quad M_{A_1} \ \to\ 0\,, \tag{7.1}$$

At the critical point, there exist three fixed points of the RGEs for a and c and each of them is associated with one of the following patterns of the chiral symmetry restoration: the Ginzburg-Landau (GL), the vector manifestation (VM) and the hybrid type. Those classes of the chiral symmetry restoration are characterized by the mass ratio, or equivalently the chiral representation mixing angle, as

$$\begin{aligned}&\text{GL-type} \ :\ \begin{cases} M_\rho^2/M_{A_1}^2 \ \to\ 1\,,\\ \cos\psi \ \to\ 0\,,\end{cases}\\ &\text{VM-type} \ :\ \begin{cases} M_\rho^2/M_{A_1}^2 \ \to\ 0\,,\\ \sin\psi \ \to\ 0\,,\end{cases}\\ &\text{Hybrid-type} \ :\ \begin{cases} M_\rho^2/M_{A_1}^2 \ \to\ 1/3\,.\\ \sin\psi \ \to\ \sqrt{\frac{1}{3}}\,.\end{cases}\end{aligned} \tag{7.2}$$

Here we study the fate of the vector dominance (VD) of the electromagnetic form factor of the pion [47] at

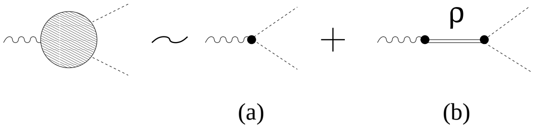

FIG. 3: Leading contributions to the electromagnetic form factor of the pion. (a) direct $\gamma\pi\pi$ and (b) $\gamma\pi\pi$ mediated by ρ-meson exchange.

the chiral symmetry restoration. The direct photon-π-π coupling $g_{\gamma\pi\pi}$ is given by

$$g_{\gamma\pi\pi} = 1 - \frac{1}{2}\frac{F_\sigma^2}{F_\pi^2}(1-\zeta^2)\,. \tag{7.3}$$

When $a = b$ and $d = 0$ are taken, this becomes

$$g_{\gamma\pi\pi} = (1-\zeta)/2\,. \tag{7.4}$$

We show the leading contributions to the pion form factor in Fig. 3. The VD is characterized by the direct $\gamma\pi\pi$ being zero. Three classes of the chiral symmetry restoration give us the following results on the VD:

$$\begin{aligned} \text{GL-type}\ &:\ g_{\gamma\pi\pi}\ \to\ 0\,,\\ \text{VM-type}\ &:\ g_{\gamma\pi\pi}\ \to\ \frac{1}{2}\,,\\ \text{Hybrid-type}\ &:\ g_{\gamma\pi\pi}\ \to\ \frac{1}{3}\,. \end{aligned} \tag{7.5}$$

In the GL-type ζ goes to 1, then the direct $\gamma\pi\pi$ goes to zero, which implies that the VD is sufficient. On the other hand, in the VM-type the direct $\gamma\pi\pi$ approaches 1/2, i.e., the VD is violated by 50%, similarly to the case of the VM [9, 18]. The hybrid type also gives about 33% violation of the VD since the direct $\gamma\pi\pi$ comes to be 1/3. This strongly affects to the understanding of the experimental data on dilepton productions based on the dropping ρ as recently pointed out in Ref. [19]. An analysis of the spectral functions taking into account of the large violation of the VD is much interesting.

Several comments are in order:

In this paper, we studied the chiral phase transition with the first and second Weinberg sum rules kept satisfied. Near the chiral restoration point in QCD with a large number of massless flavors (the large N_f QCD [48, 49]), the anomalous dimension γ_m of $\langle\bar{q}q\rangle$ becomes close to 1, $\gamma_m \sim 1$. (See, e.g., Refs. [49, 50].) This results that the term proportional to $\langle\bar{q}q\rangle^2$ in the current correlators behaves as $\sim 1/Q^4$ [51], and hence the second Weinberg sum rule is not satisfied. Thus, the condition in Eq. (5.1) is not appropriate for studying the chiral symmetry restoration in the large N_f QCD.

For studying the chiral phase transition at finite temperature using the GHLS, which is relevant to the RHIC experiment, we have to work explicitly under the existence of hot matter as done for the HLS/VM in Refs. [13, 18, 21]. Since a typical energy scale characterizing the chiral symmetry restoration, $T \sim 180\,\text{MeV}$, is much smaller than the momentum scale Q^2 in the OPE, we expect that the first and second Weinberg sum rules hold near the chiral phase transition point at finite temperature, and that the matching condition in Eq. (5.1) is applicable. Then, when the analysis in this paper is applicable to the chiral phase transition at finite temperature, we expect that the matching will produce the temperature dependence of the GHLS gauge coupling similar to the one of the HLS gauge coupling (intrinsic temperature dependence), which was essential to describe the dropping ρ occurring in the VM, and that the dropping ρ and A_1 masses are suitably described within the GHLS.

In the GHLS sector, the theory space locality is broken due to $\mathcal{O}(p^4)$ terms and we do not have the non-renormalization of the second Weinberg sum rule at one-loop. The relation between the higher order terms which generate a violation of the sum rule and the chiral symmetry restoration will be elucidated by forthcoming analysis.

In the case of the HLS, the extrapolation of the ChPT from large N_c QCD to the real-life QCD together with the Wilsonian matching reproduces several physical quantities in remarkable agreement with experiments [9, 12]. The GHLS at the leading order with a suitable parameter choice was shown [7, 29] to explain several phenomenological facts such as the successful current algebra relations $m_{A_1}^2 = 2m_\rho^2$ and $g_{A_1} = g_\rho$ [38, 52]. Furthermore, inclusion of appropriate higher order terms gives predictions on the widths of $A_1 \to \rho\pi$ and $A_1 \to \gamma\pi$ in good agreement with experiments [7, 30]. Then, we believe that the ChPT with GHLS incorporated by a suitable matching procedure will describe the low-energy phenomenology of real-life QCD. In the present analysis, we focused on the phase structure of the GHLS theory. It is interesting to study the physical quantities such as the ρ-π-π coupling and ρ-γ mixing through the matching procedure based on the ChPT with GHLS developed in this paper. We leave the analysis in the future publications.

One might think that the scalar mesons should be included, since several analysis [53] shows that they are lighter than the vector mesons in real-life QCD. For example, the analysis in Ref. [54] shows that the mass of sigma meson is about 560 MeV, which is definitely lighter than the ρ meson, $m_\rho = 770\,\text{MeV}$. In this paper, we did not include scalar meson as a dynamical degree of freedom, assuming that the light σ meson is made of two quarks and two anti-quarks [55, 56] and irrelevant to the present analysis. It is possible that another scalar meson made of $q\bar{q}$ will appear quite near the chiral restoration point and we may have to take the effects into account. Inclusion of the light scalar meson quite near the critical point may generate the quadratic divergence and change the present RGEs.

Acknowledgment

We are grateful to Yoshimasa Hidaka, Mannque Rho Masaharu Tanabashi and Koichi Yamawaki for useful discussions and comments. The work of M.H. is supported in part by the Daiko Foundation #9099, the 21st Century COE Program of Nagoya University provided by Japan Society for the Promotion of Science (15COEG01), and the JSPS Grant-in-Aid for Scientific Research (c) (2) 16540241. The work of C.S. is supported in part by the Virtual Institute of the Helmholtz Association under the grant No. VH-VI-041.

Note added

After the completion of this work, we were aware of a similar analysis by Hidaka, Morimatsu and Ohtani [57].

APPENDIX A: BACKGROUND FIELD GAUGE

In this appendix, we perform the quantization of the GHLS theory in the background field gauge.

In order that the combinations $(\phi_R \pm \phi_L)/2$ belong to the parity-eigenstates, we insert a local symmetry $H' = [SU(N_f)_V]_{\rm local}$ by dividing ξ_M into two parts as

$$\xi_M = \xi_{ML}^\dagger \cdot \xi_{MR}\,. \tag{A.1}$$

Two variables ξ_{ML} and ξ_{MR} transform as

$$\begin{aligned} &\xi_{ML} \to h' \xi_{ML} h_L^\dagger\,, \\ &\xi_{MR} \to h' \xi_{MR} h_R^\dagger\,, \end{aligned} \tag{A.2}$$

where $h' \in [SU(N_f)_V]_{\rm local}$. Accordingly we introduce the background fields $\bar\xi$ and the quantum fields $\check\xi$ as

$$\begin{aligned} &\xi_L = \bar\xi_{pL}^\dagger \check\xi_L \bar\xi_{pL} \bar\xi_L\,, \\ &\xi_R = \bar\xi_{pR}^\dagger \check\xi_R \bar\xi_{pR} \bar\xi_R\,, \\ &\xi_M = \bar\xi_{pL}^\dagger \check\xi_M \bar\xi_{pR}\,. \end{aligned} \tag{A.3}$$

The transformation properties of $\bar\xi$ and $\check\xi$ are given by

$$\begin{aligned} &\bar\xi_L \to h_L \bar\xi_L g_L^\dagger\,, \qquad \bar\xi_R \to h_R \bar\xi_R g_R^\dagger\,, \\ &\bar\xi_{pL} \to h' \bar\xi_{pL} h_L^\dagger\,, \quad \bar\xi_{pR} \to h' \bar\xi_{pR} h_R^\dagger\,, \\ &\check\xi_L \to h' \check\xi_L h'^\dagger\,, \qquad \check\xi_R \to h' \check\xi_R h'^\dagger\,, \\ &\check\xi_M \to h' \check\xi_M h'^\dagger\,, \end{aligned} \tag{A.4}$$

Then all the quantum fields transform homogeneously under the background gauge transformation:

$$(\check\pi, \check\sigma, \check q) \to h' (\check\pi, \check\sigma, \check q) h'^\dagger\,. \tag{A.5}$$

The background and quantum fields of the GHLS gauge bosons are introduced as follows:

$$\begin{aligned} &L_\mu = \bar L_\mu + g \bar\xi_{pL}^\dagger \check L_\mu \bar\xi_{pL}\,, \\ &R_\mu = \bar R_\mu + g \bar\xi_{pR}^\dagger \check R_\mu \bar\xi_{pR}\,, \end{aligned} \tag{A.6}$$

which transform as

$$\begin{aligned} &\bar L_\mu \to h_L \bar L_\mu h_L^\dagger + i h_L \partial_\mu h_L^\dagger\,, \\ &\bar R_\mu \to h_R \bar R_\mu h_R^\dagger + i h_R \partial_\mu h_R^\dagger\,, \\ &\check L_\mu \to h' \check L_\mu h'^\dagger\,, \quad \check R_\mu \to h' \check R_\mu h'^\dagger\,. \end{aligned} \tag{A.7}$$

The covariant derivatives acting on $\bar\xi$ and $\check\xi$ are expressed as

$$\begin{aligned} &\bar D_\mu \bar\xi_L = \partial_\mu \bar\xi_L - i \bar L_\mu \bar\xi_L + i \bar\xi_L \mathcal{L}_\mu \\ &\bar D_\mu \bar\xi_R = \partial_\mu \bar\xi_R - i \bar R_\mu \bar\xi_R + i \bar\xi_R \mathcal{R}_\mu \\ &\bar D_\mu \bar\xi_{pL} = \partial_\mu \bar\xi_{pL} - i \bar V'_\mu \bar\xi_{pL} + i \bar\xi_{pL} \bar L_\mu \\ &\bar D_\mu \bar\xi_{pR} = \partial_\mu \bar\xi_{pR} - i \bar V'_\mu \bar\xi_{pR} + i \bar\xi_{pR} \bar R_\mu\,, \\ &\bar D_\mu \check\xi_{L,R,M} = \partial_\mu \check\xi_{L,R,M} - i [\bar V'_\mu, \check\xi_{L,R,M}]\,, \end{aligned} \tag{A.8}$$

where $\bar V'_\mu$ is the background gauge field corresponding to the H' symmetry.

It is convenient to define the back ground fields associated with the external gauge fields as follows:

$$\begin{aligned} \bar{\mathcal{V}}_\parallel^\mu \;=\; & \frac{1}{2i}\left[\bar\xi_{pR} \partial^\mu \bar\xi_R \cdot \bar\xi_R^\dagger \bar\xi_{pR}^\dagger + \bar\xi_{pL} \partial^\mu \bar\xi_L \cdot \bar\xi_L^\dagger \bar\xi_{pL}^\dagger \right] \\ & + \frac{1}{2}\left[\bar\xi_{pR} \bar\xi_R \mathcal{R}^\mu \bar\xi_R^\dagger \bar\xi_{pR}^\dagger + \bar\xi_{pL} \bar\xi_L \mathcal{L}^\mu \bar\xi_L^\dagger \bar\xi_{pL}^\dagger \right]\,, \\ \bar{\mathcal{A}}_\perp^\mu \;=\; & \frac{1}{2i}\left[\bar\xi_{pR} \partial^\mu \bar\xi_R \cdot \bar\xi_R^\dagger \bar\xi_{pR}^\dagger - \bar\xi_{pL} \partial^\mu \bar\xi_L \cdot \bar\xi_L^\dagger \bar\xi_{pL}^\dagger \right] \\ & + \frac{1}{2}\left[\bar\xi_{pR} \bar\xi_R \mathcal{R}^\mu \bar\xi_R^\dagger \bar\xi_{pR}^\dagger - \bar\xi_{pL} \bar\xi_L \mathcal{L}^\mu \bar\xi_L^\dagger \bar\xi_{pL}^\dagger \right]\,. \end{aligned} \tag{A.9}$$

Furthermore, we use

$$\begin{aligned} &\bar V_\mu = \frac{1}{2}\left[\bar\xi_{pR} \bar R_\mu \bar\xi_{pR}^\dagger + \bar\xi_{pL} \bar L_\mu \bar\xi_{pL}^\dagger \right]\,, \\ &\bar A_\mu = \frac{1}{2}\left[\bar\xi_{pR} \bar R_\mu \bar\xi_{pR}^\dagger - \bar\xi_{pL} \bar L_\mu \bar\xi_{pL}^\dagger \right]\,, \end{aligned} \tag{A.10}$$

and

$$\begin{aligned} \bar{\mathcal{V}}_M^\mu \;=\; & \frac{1}{2i}\left[\partial^\mu \bar\xi_{pR} \cdot \bar\xi_{pR}^\dagger + \partial^\mu \bar\xi_{pL} \cdot \bar\xi_{pL}^\dagger \right]\,, \\ \bar{\mathcal{A}}_M^\mu \;=\; & \frac{1}{2i}\left[\partial^\mu \bar\xi_{pR} \cdot \bar\xi_{pR}^\dagger - \partial^\mu \bar\xi_{pL} \cdot \bar\xi_{pL}^\dagger \right]\,. \end{aligned} \tag{A.11}$$

We fix the background field gauge as

$$\mathcal{L}_{\rm GF}^{(V+A)} = -\frac{1}{\alpha}\,{\rm tr}\left[F_V^2 + F_A^2 \right]\,, \tag{A.12}$$

where α is the gauge fixing parameter, and F_V and F_A are defined as

$$\begin{aligned} F_V \;=\; & \bar D^\mu \check V_\mu + \alpha g F_\sigma^2 \check\phi_\sigma + i\left[\bar V'^\mu - \bar V^\mu - \bar{\mathcal{V}}_M^\mu\,,\, \check V_\mu \right] \\ & - i\left[\bar A^\mu + \bar{\mathcal{A}}_M^\mu\,,\, \check A_\mu \right]\,, \\ F_A \;=\; & \bar D^\mu \check A_\mu - \alpha g F_q^2 \check\phi_q + i\left[\bar V'^\mu - \bar V^\mu - \bar{\mathcal{V}}_M^\mu\,,\, \check A_\mu \right] \\ & - i\left[\bar A^\mu + \bar{\mathcal{A}}_M^\mu\,,\, \check V_\mu \right]\,, \end{aligned} \tag{A.13}$$

with $\bar{D}^\mu$ denoting the covariant derivative in terms of the background fields:

$$\begin{aligned}\bar{D}_\mu \check{V}^\nu &= \partial_\mu \check{V}^\nu - i[\bar{V}'_\mu, \check{V}^\nu]\,,\\ \bar{D}_\mu \check{A}^\nu &= \partial_\mu \check{A}^\nu - i[\bar{V}'_\mu, \check{A}^\nu]\,. \end{aligned}\qquad (A.14)$$

The FP ghost Lagrangian associated with $\mathcal{L}_{\rm GF}$ is given by

$$\begin{aligned}\mathcal{L}_{\rm FP}^{(V+A)} &= 2i{\rm tr}\Big[\bar{C}_V\Big\{\bar{D}_\mu\Big(\bar{D}^\mu C_V + \alpha g^2 F_\sigma^2 C_V\\ &\quad - i[\bar{V}'^\mu - \bar{V}^\mu - \bar{\mathcal{V}}_M^\mu, C_V] - i[\bar{A}^\mu + \bar{\mathcal{A}}_M^\mu, C_A]\Big)\Big\}\Big]\\ &\quad + 2i{\rm tr}\Big[\bar{C}_A\Big\{\bar{D}_\mu\Big(\bar{D}^\mu C_A + \alpha g^2 F_q^2 C_A\\ &\qquad - i[\bar{V}'^\mu - \bar{V}^\mu - \bar{\mathcal{V}}_M^\mu, C_A] - i[\bar{A}^\mu + \bar{\mathcal{A}}_M^\mu, C_V]\Big)\Big\}\Big]\\ &\quad - 2{\rm tr}\Big[\Big\{[\bar{V}'^\mu - \bar{V}^\mu - \bar{\mathcal{V}}_M^\mu, \bar{C}_V] + [\bar{A}^\mu + \bar{\mathcal{A}}_M^\mu, \bar{C}_A]\Big\}\\ &\quad \times\Big\{\bar{D}_\mu C_V - i[\bar{V}'^\mu - \bar{V}^\mu - \bar{\mathcal{V}}_M^\mu, C_V]\\ &\qquad - i[\bar{A}^\mu + \bar{\mathcal{A}}_M^\mu, C_A]\Big\}\Big]\\ &\quad - 2{\rm tr}\Big[\Big\{[\bar{V}'^\mu - \bar{V}^\mu - \bar{\mathcal{V}}_M^\mu, \bar{C}_A] + [\bar{A}^\mu + \bar{\mathcal{A}}_M^\mu, \bar{C}_V]\Big\}\\ &\quad \times\Big\{\bar{D}_\mu C_A - i[\bar{V}'^\mu - \bar{V}^\mu - \bar{\mathcal{V}}_M^\mu, C_A]\\ &\qquad - i[\bar{A}^\mu + \bar{\mathcal{A}}_M^\mu, C_V]\Big\}\Big] + \cdots\,, \end{aligned}\qquad (A.15)$$

where ellipses stand for the terms including at least three quantum fields.

Finally, we should eliminate the redundant H' symmetry. This can be done by relating $\bar{V}'_\mu$ to other background fields. In this paper we take

$$\bar{V}'^\mu = \bar{\mathcal{V}}_M^\mu + \bar{V}^\mu\,. \qquad (A.16)$$

and set $\bar{\xi}_{pL} = \bar{\xi}_{pR} \equiv \bar{\xi}_p$. We should note that the background field $\bar{V}'_\mu$ appears only in $\mathcal{L}_{\rm GF} + \mathcal{L}_{\rm FP}$ given in Eqs. (A.12) and (A.15), and is not included in the Lagrangian in Eq. (2.12).

APPENDIX B: QUANTUM CORRECTIONS

In this appendix, we list the quantum corrections to the two-point functions and the RGEs at one loop. In the present analysis, we adopt the 't Hooft-Feynman gauge by taking $\alpha = 1$ in Eqs. (A.12) and (A.15).

For expressing the quantum corrections in simple forms it is convenient to define the following Feynman integrals:

$$\begin{aligned} A_0(M) &= \int \frac{d^n k}{i(2\pi)^4}\frac{1}{M^2 - k^2}\,,\\ B_0(p;M_1,M_2)&\\ &= \int \frac{d^n k}{i(2\pi)^4}\frac{1}{[M_1^2 - k^2][M_2^2-(k-p)^2]}\,,\\ B^{\mu\nu}(p;M_1,M_2)&\\ &= \int \frac{d^n k}{i(2\pi)^4}\frac{(2k-p)^\mu(2k-p)^\nu}{[M_1^2 - k^2][M_2^2-(k-p)^2]}\,. \end{aligned}\qquad (B.1)$$

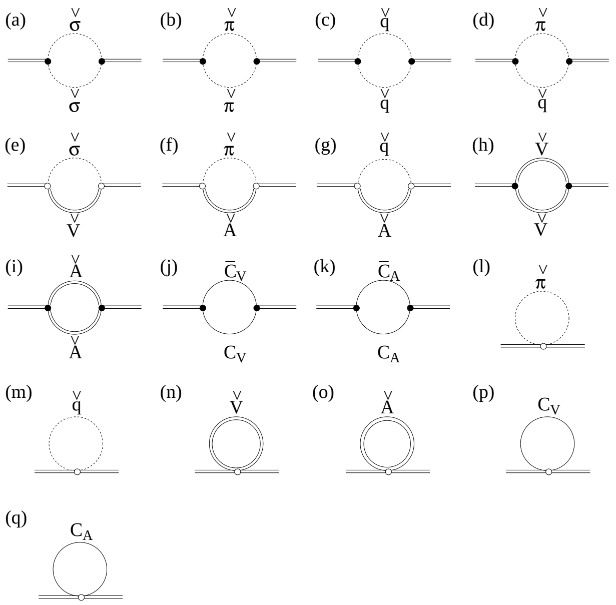

FIG. 4: Diagrams for contributions to $\Pi^{\mu\nu}_{\bar{V}\bar{V}}$ at one loop. The circle (○) denotes the momentum-independent vertex and the dot (●) denotes the momentum-dependent vertex.

We take into account the quadratic as well as the logarithmic divergences following Eqs. (3.3) and (3.4), which preserve the chiral symmetry. Here we summarize the divergent parts of the above Feynman integrals:

$$\begin{aligned} A_0(M)|_{\rm div} &= \frac{\Lambda^2}{(4\pi)^2} - \frac{M^2}{(4\pi)^2}\ln\Lambda^2\,,\\ B_0(p;M_1,M_2)|_{\rm div} &= \frac{1}{(4\pi)^2}\ln\Lambda^2\,,\\ B^{\mu\nu}(p;M_1,M_2)|_{\rm div}&\\ = -g^{\mu\nu}\frac{1}{(4\pi)^2}&\left[2\Lambda^2 - \left(M_1^2+M_2^2\right)\ln\Lambda^2\right]\\ &- \left(p^2 g^{\mu\nu} - p^\mu p^\nu\right)\frac{1}{3(4\pi)^2}\ln\Lambda^2\,. \end{aligned}\qquad (B.2)$$

The quantum corrections to $\Pi^{\mu\nu}_{\bar{V}\bar{V}}$ generated by the loop diagrams shown in Fig. 4 are given by

$$
\begin{aligned}
\Pi^{(\mathrm{a})\mu\nu}_{\bar V\bar V} &= \frac{N_f}{8} B^{\mu\nu}(p;M_\rho,M_\rho)\,,\\
\Pi^{(\mathrm{b})\mu\nu}_{\bar V\bar V} &= \frac{N_f}{8}\left(\frac{F}{F_\pi}\right)^4 a^2(1-\zeta)^2(1+\zeta)^2 B^{\mu\nu}(p;0,0)\,,\\
\Pi^{(\mathrm{c})\mu\nu}_{\bar V\bar V} &= \frac{N_f}{8}\left(\frac{F}{F_q}\right)^4 [a-2(b+c)]^2 B^{\mu\nu}(p;M_{A_1},M_{A_1})\,,\\
\Pi^{(\mathrm{d})\mu\nu}_{\bar V\bar V} &= \frac{N_f}{4}\left(\frac{F^2}{F_\pi F_q}\right)^2 (a\zeta-b)^2 B^{\mu\nu}(p;M_{A_1},0)\,,\\
\Pi^{(\mathrm{e})\mu\nu}_{\bar V\bar V} &= -N_f M_\rho^2 g^{\mu\nu} B_0(p;M_\rho,M_\rho)\,,\\
\Pi^{(\mathrm{f})\mu\nu}_{\bar V\bar V} &= -N_f\left(\frac{F}{F_\pi}\right)^2 g^2F^2(a\zeta-b)^2\\
&\quad \times g^{\mu\nu}B_0(p;M_{A_1},0)\,,\\
\Pi^{(\mathrm{g})\mu\nu}_{\bar V\bar V} &= -N_f\left(\frac{F}{F_q}\right)^2 g^2a^2F^2 g^{\mu\nu}B_0(p;M_{A_1},M_{A_1})\,,\\
\Pi^{(\mathrm{h})\mu\nu}_{\bar V\bar V} &= \frac{N_f}{2}\Big[nB^{\mu\nu}(p;M_\rho,M_\rho)\\
&\quad + 8(p^2g^{\mu\nu}-p^\mu p^\nu)B_0(p;M_\rho,M_\rho)\Big]\,,\\
\Pi^{(\mathrm{i})\mu\nu}_{\bar V\bar V} &= \frac{N_f}{2}\Big[nB^{\mu\nu}(p;M_{A_1},M_{A_1})\\
&\quad + 8(p^2g^{\mu\nu}-p^\mu p^\nu)B_0(p;M_{A_1},M_{A_1})\Big]\,,\\
\Pi^{(\mathrm{j})\mu\nu}_{\bar V\bar V} &= -N_f B^{\mu\nu}(p;M_\rho,M_\rho)\,,\\
\Pi^{(\mathrm{k})\mu\nu}_{\bar V\bar V} &= -N_f B^{\mu\nu}(p;M_{A_1},M_{A_1})\,,\\
\Pi^{(\mathrm{l})\mu\nu}_{\bar V\bar V} &= -N_f\left(\frac{F}{F_\pi}\right)^2 \zeta(a\zeta-b)g^{\mu\nu}A_0(0)\,,\\
\Pi^{(\mathrm{m})\mu\nu}_{\bar V\bar V} &= N_f\left(\frac{F}{F_q}\right)^4 (a-b-c)^2 g^{\mu\nu}A_0(M_{A_1})\,,\\
\Pi^{(\mathrm{n})\mu\nu}_{\bar V\bar V} &= N_f n\, g^{\mu\nu}A_0(M_\rho)\,,\\
\Pi^{(\mathrm{o})\mu\nu}_{\bar V\bar V} &= N_f n\, g^{\mu\nu}A_0(M_{A_1})\,,\\
\Pi^{(\mathrm{p})\mu\nu}_{\bar V\bar V} &= -2N_f g^{\mu\nu}A_0(M_\rho)\,,\\
\Pi^{(\mathrm{q})\mu\nu}_{\bar V\bar V} &= -2N_f g^{\mu\nu}A_0(M_{A_1})\,,
\end{aligned}
\tag{B.3}
$$

where n denotes the dimension of the spacetime. We show the one-loop diagrams to contribute to $\Pi^{\mu\nu}_{\bar A\bar A}$ in Fig. 5. We obtain the quantum corrections as

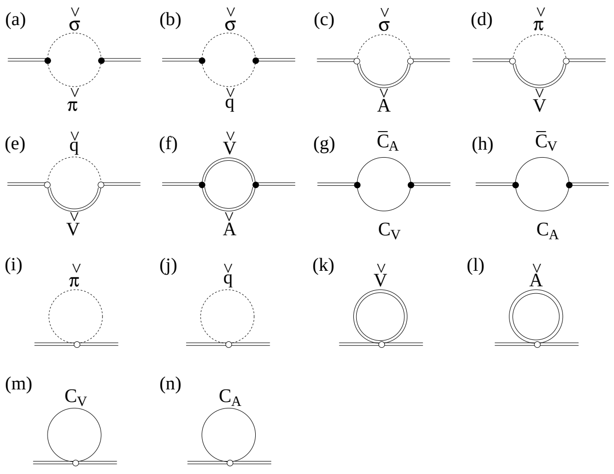

FIG. 5: Diagrams for contributions to $\Pi^{\mu\nu}_{\bar A\bar A}$ at one loop.

$$
\begin{aligned}
\Pi^{(\mathrm{a})\mu\nu}_{\bar A\bar A} &= \frac{N_f}{4}\left(\frac{F^2}{F_\sigma F_\pi}\right)^2 (a\zeta-b)^2 B^{\mu\nu}(p;M_\rho,0)\,,\\
\Pi^{(\mathrm{b})\mu\nu}_{\bar A\bar A} &= \frac{N_f}{4}a^2\left(\frac{F^2}{F_\sigma F_q}\right)^2 B^{\mu\nu}(p;M_\rho,M_{A_1})\,,\\
\Pi^{(\mathrm{c})\mu\nu}_{\bar A\bar A} &= -N_f M_\rho^2 g^{\mu\nu}B_0(p;M_\rho,M_{A_1})\,,\\
\Pi^{(\mathrm{d})\mu\nu}_{\bar A\bar A} &= -N_f\left(\frac{F}{F_\pi}\right)^2 g^2F^2\zeta^2(a-b-c)^2\\
&\quad \times g^{\mu\nu}B_0(p;M_\rho,0)\,,\\
\Pi^{(\mathrm{e})\mu\nu}_{\bar A\bar A} &= -N_f\left(\frac{F}{F_q}\right)^2 g^2F^2[a-2(b+c)]^2\\
&\quad \times g^{\mu\nu}B_0(p;M_\rho,M_{A_1})\,,\\
\Pi^{(\mathrm{f})\mu\nu}_{\bar A\bar A} &= N_f\Big[nB^{\mu\nu}(p;M_\rho,M_{A_1})\\
&\quad + 8(p^2g^{\mu\nu}-p^\mu p^\nu)B_0(p;M_\rho,M_{A_1})\Big]\,,\\
\Pi^{(\mathrm{g})\mu\nu}_{\bar A\bar A} &= -N_f B^{\mu\nu}(p;M_\rho,M_{A_1})\,,\\
\Pi^{(\mathrm{h})\mu\nu}_{\bar A\bar A} &= -N_f B^{\mu\nu}(p;M_\rho,M_{A_1})\,,\\
\Pi^{(\mathrm{i})\mu\nu}_{\bar A\bar A} &= N_f\left(\frac{F}{F_\pi}\right)^2 (a-b-c)\zeta^2 g^{\mu\nu}A_0(0)\,,\\
\Pi^{(\mathrm{j})\mu\nu}_{\bar A\bar A} &= N_f\left(\frac{F}{F_q}\right)^2 (a-b-c)g^{\mu\nu}A_0(M_{A_1})\,,\\
\Pi^{(\mathrm{k})\mu\nu}_{\bar A\bar A} &= N_f n\, g^{\mu\nu}A_0(M_\rho)\,,\\
\Pi^{(\mathrm{l})\mu\nu}_{\bar A\bar A} &= N_f n\, g^{\mu\nu}A_0(M_{A_1})\,,\\
\Pi^{(\mathrm{m})\mu\nu}_{\bar A\bar A} &= -2N_f g^{\mu\nu}A_0(M_\rho)\,,\\
\Pi^{(\mathrm{n})\mu\nu}_{\bar A\bar A} &= -2N_f g^{\mu\nu}A_0(M_{A_1})\,.
\end{aligned}
\tag{B.4}
$$

From the diagrams shown in Fig. 6, we obtain

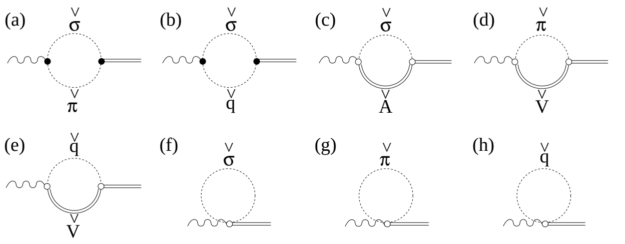

FIG. 6: Diagrams for contributions to $\Pi^{\mu\nu}_{\bar{\mathcal{A}}_\perp \bar{A}}$ at one loop.

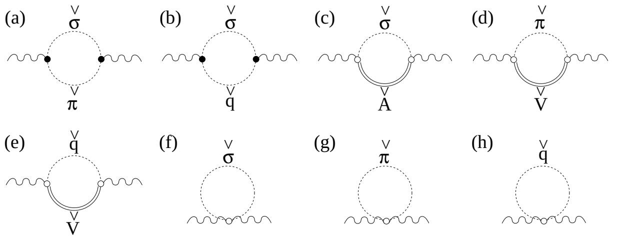

FIG. 7: Diagrams for contributions to $\Pi^{\mu\nu}_{\bar{A}_M \bar{\mathcal{A}}_\perp}$ at one loop.

$$
\begin{aligned}
\Pi^{(\mathrm{a})\mu\nu}_{\bar{\mathcal{A}}_\perp \bar{A}} &= -\frac{N_f}{4}\Big(\frac{F^2}{F_\sigma F_\pi}\Big)^2 (a-b\zeta) \\
&\quad \times (a\zeta - b) B^{\mu\nu}(p; M_\rho, 0)\,, \\
\Pi^{(\mathrm{b})\mu\nu}_{\bar{\mathcal{A}}_\perp \bar{A}} &= \frac{N_f}{4}\Big(\frac{F^2}{F_\sigma F_q}\Big)^2 ab B^{\mu\nu}(p; M_\rho, M_{A_1})\,, \\
\Pi^{(\mathrm{c})\mu\nu}_{\bar{\mathcal{A}}_\perp \bar{A}} &= N_f\Big(\frac{F}{F_\sigma}\Big)^2 g^2 F^2 ab g^{\mu\nu} B_0(p; M_\rho, M_{A_1})\,, \\
\Pi^{(\mathrm{d})\mu\nu}_{\bar{\mathcal{A}}_\perp \bar{A}} &= N_f\Big(\frac{F}{F_\pi}\Big)^2 g^2 F^2 \zeta(a-b\zeta) \\
&\quad \times (a-b-c) g^{\mu\nu} B_0(p; M_\rho, 0)\,, \\
\Pi^{(\mathrm{e})\mu\nu}_{\bar{\mathcal{A}}_\perp \bar{A}} &= -N_f\Big(\frac{F}{F_q}\Big)^2 g^2 F^2 b[a-2(b+c)] \\
&\quad \times g^{\mu\nu} B_0(p; M_\rho, M_{A_1})\,, \\
\Pi^{(\mathrm{f})\mu\nu}_{\bar{\mathcal{A}}_\perp \bar{A}} &= \frac{N_f}{2}\Big(\frac{F}{F_\sigma}\Big)^2 b g^{\mu\nu} A_0(M_\rho)\,, \\
\Pi^{(\mathrm{g})\mu\nu}_{\bar{\mathcal{A}}_\perp \bar{A}} &= N_f\Big(\frac{F}{F_\pi}\Big)^2 \Big[-a\zeta + b\Big(1-\frac{1}{2}(1-\zeta^2)\Big)\Big] \\
&\quad \times g^{\mu\nu} A_0(0)\,, \\
\Pi^{(\mathrm{h})\mu\nu}_{\bar{\mathcal{A}}_\perp \bar{A}} &= \frac{N_f}{2}\Big(\frac{F}{F_q}\Big)^2 b g^{\mu\nu} A_0(M_{A_1})\,. \qquad \text{(B.5)}
\end{aligned}
$$

Finally we list the quantum corrections contributing to $\Pi^{\mu\nu}_{\bar{A}_M \bar{\mathcal{A}}_\perp}$ shown in Fig. 7:

$$
\begin{aligned}
\Pi^{(\mathrm{a})\mu\nu}_{\bar{A}_M \bar{\mathcal{A}}_\perp} &= \frac{N_f}{4}\Big(\frac{F^2}{F_\sigma F_\pi}\Big)^2 (1-\zeta)(a+b)(a-b\zeta) \\
&\quad \times B^{\mu\nu}(p; M_\rho, 0)\,, \\
\Pi^{(\mathrm{b})\mu\nu}_{\bar{A}_M \bar{\mathcal{A}}_\perp} &= \frac{N_f}{4}\Big(\frac{F^2}{F_\sigma F_q}\Big)^2 b(a+b) B^{\mu\nu}(p; M_\rho, M_{A_1})\,, \\
\Pi^{(\mathrm{c})\mu\nu}_{\bar{A}_M \bar{\mathcal{A}}_\perp} &= N_f\Big(\frac{F}{F_\sigma}\Big)^2 g^2 F^2 b(a-b) \\
&\quad \times g^{\mu\nu} B_0(p; M_\rho, M_{A_1})\,, \\
\Pi^{(\mathrm{d})\mu\nu}_{\bar{A}_M \bar{\mathcal{A}}_\perp} &= -N_f\Big(\frac{F}{F_\pi}\Big)^2 g^2 F^2 (a-b\zeta) \\
&\quad \times [a(1-\zeta) + c\zeta] g^{\mu\nu} B_0(p; M_\rho, 0)\,, \\
\Pi^{(\mathrm{e})\mu\nu}_{\bar{A}_M \bar{\mathcal{A}}_\perp} &= -N_f\Big(\frac{F}{F_q}\Big)^2 g^2 F^2 b(a-b-2c) \\
&\quad \times g^{\mu\nu} B_0(p; M_\rho, M_{A_1})\,, \\
\Pi^{(\mathrm{f})\mu\nu}_{\bar{A}_M \bar{\mathcal{A}}_\perp} &= \frac{N_f}{2}\Big(\frac{F}{F_\sigma}\Big)^2 b g^{\mu\nu} A_0(M_\rho)\,, \\
\Pi^{(\mathrm{g})\mu\nu}_{\bar{A}_M \bar{\mathcal{A}}_\perp} &= \frac{N_f}{2}\Big(\frac{F}{F_\pi}\Big)^2 [\,2a(1-\zeta) - b(1-\zeta^2) - 2d\,] \\
&\quad \times g^{\mu\nu} A_0(0)\,, \\
\Pi^{(\mathrm{h})\mu\nu}_{\bar{A}_M \bar{\mathcal{A}}_\perp} &= \frac{N_f}{2}\Big(\frac{F}{F_q}\Big)^2 b g^{\mu\nu} A_0(M_{A_1})\,. \qquad \text{(B.6)}
\end{aligned}
$$

The quadratic and logarithmic divergences generated by those diagrams are renormalized following Eq. (3.8).

The renormalization group equations (RGEs) for the leading order parameters (a, b, c, d and g) take the following forms:

$$
\begin{aligned}
\mu\frac{d(aF^2)}{d\mu} &= \frac{N_f}{(4\pi)^2}\Bigg[\mu^2\Big\{\frac{1}{2} + \frac{1}{2}\Big(\frac{F}{F_\pi}\Big)^4 a^2(1-\zeta^2)^2 \\
&+ \frac{1}{2}\Big(\frac{F}{F_q}\Big)^4 [a-2(b+c)]^2 + \Big(\frac{F^2}{F_\pi F_q}\Big)^2 (a\zeta-b)^2 \\
&+ 2\Big(\frac{F}{F_\pi}\Big)^2 \zeta(a\zeta-b) + 2\Big(\frac{F}{F_q}\Big)^2 (a-b-c)\Big\} \\
&+ \frac{3}{2}M_\rho^2 + 2\Big(\frac{F}{F_q}\Big)^2 a M_\rho^2 + 2\Big(\frac{F}{F_\pi}\Big)^2 g^2 F^2 (a\zeta-b)^2 \\
&- 2\Big(\frac{F}{F_q}\Big)^2 (a-b-c) M_{A_1}^2 - \frac{1}{2}\Big(\frac{F}{F_q}\Big)^4 [a-2(b+c)]^2 M_{A_1}^2 \\
&- \frac{1}{2}\Big(\frac{F^2}{F_\pi F_q}\Big)^2 (a\zeta-b)^2 M_{A_1}^2\Bigg]\,, \qquad \text{(B.7)}
\end{aligned}
$$

$$\begin{aligned}
\mu\frac{d(bF^2)}{d\mu} = \frac{N_f}{(4\pi)^2}\Bigg[&\mu^2\Big\{\Big(\frac{F}{F_\sigma}\Big)^2 b \\
&+ 2\Big(\frac{F}{F_\pi}\Big)^2\big[-a\zeta + b\big(1-\frac{1}{2}(1-\zeta^2)\big)\big] \\
&+ \Big(\frac{F^2}{F_\sigma F_\pi}\Big)^2 (a-b\zeta)(a\zeta-b)\Big\} \\
&+ \Big(\frac{F}{F_\sigma}\Big)^2 b M_\rho^2 - 2\Big(\frac{F}{F_q}\Big)^2 b\big(M_\rho^2 - \frac{3}{2}M_{A_1}^2\big) \\
&+ 2\Big(\frac{F}{F_\pi}\Big)^2 \zeta(a-b\zeta)(M_\rho^2 - M_{A_1}^2) \\
&- \frac{1}{2}\Big(\frac{F^2}{F_\sigma F_\pi}\Big)^2 (a-b\zeta)(a\zeta-b)M_\rho^2 \\
&+ \frac{1}{2}\Big(\frac{F^2}{F_\sigma F_q}\Big)^2 ab(M_\rho^2 + M_{A_1}^2)\Bigg]\,,
\end{aligned} \tag{B.8}$$

$$\begin{aligned}
\mu\frac{d(cF^2)}{d\mu} = \frac{N_f}{(4\pi)^2}\Bigg[&\mu^2\Big\{-\Big(\frac{F}{F_\sigma}\Big)^2 b \\
&- 2\Big(\frac{F}{F_\pi}\Big)^2\big[-a\zeta(1-\zeta) + \frac{1}{2}b(1-\zeta^2) - c\zeta^2\big] \\
&- \Big(\frac{F}{F_q}\Big)^2 (a-b-2c) + \Big(\frac{F^2}{F_\sigma F_q}\Big)^2 ab \\
&- \Big(\frac{F^2}{F_\sigma F_\pi}\Big)^2 (a+b)(1-\zeta)(a\zeta-b)\Big\} \\
&+ \Big(\frac{F}{F_\sigma}\Big)^2 (2a-b)M_\rho^2 \\
&- 2\Big(\frac{F}{F_\pi}\Big)^2 \zeta[a(1-\zeta)+c\zeta](M_\rho^2 - M_{A_1}^2) \\
&+ 2\Big(\frac{F}{F_q}\Big)^2\Big[\Big(\frac{3}{4}a - b - 2c\Big)M_\rho^2 \\
&\qquad + \Big(-\frac{5}{4}a + \frac{3}{2}b + 3c\Big)M_{A_1}^2\Big] \\
&+ \frac{1}{2}\Big(\frac{F^2}{F_\sigma F_\pi}\Big)^2 (a+b)(1-\zeta)(a\zeta-b)M_\rho^2 \\
&- \frac{1}{2}\Big(\frac{F^2}{F_\sigma F_q}\Big)^2 ab(M_\rho^2 + M_{A_1}^2)\Bigg]\,,
\end{aligned} \tag{B.9}$$

$$\begin{aligned}
\mu\frac{d(dF^2)}{d\mu} = \frac{N_f}{(4\pi)^2}\Bigg[&\mu^2\Big\{-\Big(\frac{F}{F_\sigma}\Big)^2 b \\
&- \Big(\frac{F}{F_\pi}\Big)^2 [2a(1-\zeta) - b(1-\zeta^2) - 2d] \\
&- \Big(\frac{F}{F_q}\Big)^2 b + \Big(\frac{F^2}{F_\sigma F_\pi}\Big)^2 (a+b)(1-\zeta)(a-b\zeta) \\
&+ \Big(\frac{F^2}{F_\sigma F_q}\Big)^2 b(a+b)\Big\} - 2\Big(\frac{F}{F_\sigma}\Big)^2 g^2F^2 b\Big(\frac{1}{2}a - b\Big) \\
&+ 2\Big(\frac{F}{F_\pi}\Big)^2 g^2F^2(a-b\zeta)[a(1-\zeta)+c\zeta] \\
&+ 2\Big(\frac{F}{F_q}\Big)^2 g^2F^2 b\Big(a - \frac{1}{2}b - \frac{3}{2}c\Big) \\
&- \frac{1}{2}\Big(\frac{F^2}{F_\sigma F_\pi}\Big)^2 (a+b)(1-\zeta)(a-b\zeta)M_\rho^2 \\
&- \frac{1}{2}\Big(\frac{F^2}{F_\sigma F_q}\Big)^2 b(a+b)(M_\rho^2 + M_{A_1}^2)\Bigg]\,,
\end{aligned} \tag{B.10}$$

$$\begin{aligned}
\mu\frac{dg^2}{d\mu} = \frac{N_f}{(4\pi)^2}\frac{1}{12}\Bigg[&-\frac{351}{2} + \Big(\frac{F}{F_q}\Big)^2 a \\
&+ \frac{1}{2}\Big(\frac{F}{F_\pi}\Big)^4 a^2(1-\zeta^2)^2 + \frac{1}{2}\Big(\frac{F}{F_q}\Big)^4 [a-2(b+c)]^2 \\
&+ \Big(\frac{F^2}{F_\sigma F_\pi}\Big)^2 (a\zeta-b)^2 + \Big(\frac{F^2}{F_\pi F_q}\Big)^2 (a\zeta-b)^2\Bigg] g^4\,,
\end{aligned} \tag{B.11}$$

where μ denotes a renormalization scale.

When we take the parameter choice satisfying $a = b$ and $d = 0$, the RGEs are reduced to

$$\begin{aligned}
\mu\frac{d(aF^2)}{d\mu} &= \frac{N_f}{(4\pi)^2}\Big[\mu^2 + 3ag^2F^2\Big]\,, \\
\mu\frac{d(bF^2)}{d\mu} &= \frac{N_f}{(4\pi)^2}\Big[\mu^2 + 3ag^2F^2\Big]\,, \\
\mu\frac{d(cF^2)}{d\mu} &= \frac{N_f}{(4\pi)^2}\Big[2\mu^2 + 6cg^2F^2\Big]\,, \\
\mu\frac{d(dF^2)}{d\mu} &= 0\,, \\
\mu\frac{dg^2}{d\mu} &= -\frac{N_f}{(4\pi)^2}\frac{43}{3}g^4\,.
\end{aligned} \tag{B.12}$$

---

[1] See, e.g., V. Bernard and U. G. Meissner, Nucl. Phys. A **489**, 647 (1988); T. Hatsuda and T. Kunihiro, Phys. Rept. **247**, 221 (1994) [hep-ph/9401310]; R. D. Pisarski, hep-ph/9503330; R. Rapp and J. Wambach, Adv. Nucl. Phys. **25**, 1 (2000). F. Wilczek, hep-ph/0003183. G. E. Brown and M. Rho, Phys. Rept. **363**, 85 (2002) [arXiv:hep-ph/0103102];

[2] G. E. Brown and M. Rho, Phys. Rev. Lett. **66**, 2720 (1991).

[3] G. Q. Li, C. M. Ko and G. E. Brown, Phys. Rev. Lett. **75**, 4007 (1995).

[4] G. Agakishiev *et al.* [CERES Collaboration], Phys. Rev. Lett. **75**, 1272 (1995).

[5] M. Harada and K. Yamawaki, Phys. Rev. Lett. **86**, 757 (2001) [arXiv:hep-ph/0010207].

[6] M. Bando, T. Kugo, S. Uehara, K. Yamawaki and T. Yanagida, Phys. Rev. Lett. **54**, 1215 (1985).

[7] M. Bando, T. Kugo and K. Yamawaki, Phys. Rept. **164**, 217 (1988).

[8] M. Harada and K. Yamawaki, Phys. Lett. B **297**, 151 (1992) [arXiv:hep-ph/9210208].

[9] M. Harada and K. Yamawaki, Phys. Rept. **381**, 1 (2003) [arXiv:hep-ph/0302103].

[10] H. Georgi, Phys. Rev. Lett. **63** (1989) 1917; Nucl. Phys. B **331**, 311 (1990).

[11] M. Tanabashi, Phys. Lett. B **316**, 534 (1993)

[12] M. Harada and K. Yamawaki, Phys. Rev. D **64** 014023 (2001) [arXiv:hep-ph/0009163].

[13] M. Harada and C. Sasaki, Phys. Lett. B **537**, 280 (2002) [arXiv:hep-ph/0109034].

[14] M. Harada, Y. Kim and M. Rho, Phys. Rev. D **66**, 016003 (2002) [arXiv:hep-ph/0111120].

[15] K. Ozawa *et al.* [E325 Collaboration], Phys. Rev. Lett. **86**, 5019 (2001); S. Yokkaichi, Talk given at International Workshop on "Chiral Restoration in Nuclear Medium", February 15 - 17, 2005, RIKEN, Japan (http://chiral05.riken.jp/); M. Naruki *et al.*, arXiv:nucl-ex/0504016.

[16] D. Trnka *et al.* [CBELSA/TAPS Collaboration], Phys. Rev. Lett. **94**, 192303 (2005).

[17] E. V. Shuryak and G. E. Brown, Nucl. Phys. A **717**, 322 (2003).

[18] M. Harada and C. Sasaki, Nucl. Phys. A **736**, 300 (2004) [arXiv:hep-ph/0304282].

[19] G. E. Brown and M. Rho, arXiv:nucl-th/0509001; arXiv:nucl-th/0509002.

[20] See, e.g., the talks presented at the Quark Matter 2005: E. Scomparin, S. Damjanovici, L. Maiani, I. Tserruya and C. Gale.

[21] C. Sasaki, Nucl. Phys. A **739**, 151 (2004) [arXiv:hep-ph/0306005]; M. Harada, Y. Kim, M. Rho and C. Sasaki, Nucl. Phys. A **730**, 379 (2004) [arXiv:hep-ph/0308237]; M. Harada, M. Rho and C. Sasaki, arXiv:hep-ph/0506092.

[22] J. G. Cramer, G. A. Miller, J. M. S. Wu and J. H. S. Yoon, Phys. Rev. Lett. **94**, 102302 (2005).

[23] J. Adams *et al.* [STAR Collaboration], arXiv:nucl-ex/0411036; Phys. Rev. Lett. **92**, 112301 (2004).

[24] G. E. Brown, C. H. Lee and M. Rho, arXiv:nucl-th/0507073.

[25] J. Adams *et al.* [STAR Collaboration], Phys. Rev. Lett. **92**, 092301 (2004) [arXiv:nucl-ex/0307023].

[26] See, e.g., C. Song and V. Koch, Phys. Lett. B **404**, 1 (1997) [arXiv:nucl-th/9703010]; M. Urban, M. Buballa and J. Wambach, Phys. Rev. Lett. **88**, 042002 (2002) [arXiv:nucl-th/0110005].

[27] See, e.g., J. Schwinger, Phys. Lett. B **24**, 473 (1967); J. Schwinger, Paticles and Sourses (Gordon and Greach, New York, 1969); J. Wess and B. Zumino, Phys. Rev. **163**, 1727 (1967); S. Gasiorowicz and D. A. Geffen, Rev. Mod. Phys. **41**, 531 (1969); O. Kaymakcalan, S. Rajeev and J. Schechter, Phys. Rev. D **30**, 594 (1984); and Ref. [58].

[28] J. Gasser and H. Leutwyler, Annals Phys. **158**, 142 (1984); G. Ecker, J. Gasser, A. Pich and E. de Rafael, Nucl. Phys. B **321**, 311 (1989).

[29] M. Bando, T. Kugo and K. Yamawaki, Nucl. Phys. B **259**, 493 (1985).

[30] M. Bando, T. Fujiwara and K. Yamawaki, Prog. Theor. Phys. **79**, 1140 (1988).

[31] N. Kaiser and U. G. Meissner, Nucl. Phys. A **519**, 671 (1990).

[32] See, e.g., K. Yamawaki, Phys. Rev. D **35**, 412 (1987); U. G. Meissner and I. Zahed, Z. Phys. A **327**, 5 (1987); M. F. Golterman and N. D. Hari Dass, Nucl. Phys. B **277**, 739 (1986); G. Ecker, J. Gasser, H. Leutwyler, A. Pich and E. de Rafael, Phys. Lett. B **223**, 425 (1989); M. Tanabashi, Phys. Lett. B **384**, 218 (1996); and also Refs. [7, 9, 58].

[33] J. Gasser and H. Leutwyler, Annals Phys. **158**, 142 (1984).

[34] J. Gasser and H. Leutwyler, Nucl. Phys. B **250**, 517 (1985).

[35] M. Harada and K. Yamawaki, Phys. Rev. Lett. **83**, 3374 (1999) [arXiv:hep-ph/9906445].

[36] M. Veltman, Acta Phys. Polon. B **12**, 437 (1981).

[37] Y. L. Ma, Q. Wang and Y. L. Wu, Eur. Phys. J. C **39**, 201 (2005) [arXiv:hep-ph/0411078].

[38] M. A. Shifman, A. I. Vainshtein and V. I. Zakharov, Nucl. Phys. B **147**, 385 (1979); Nucl. Phys. B **147**, 448 (1979).

[39] S. Weinberg, Phys. Rev. Lett. **18**, 507 (1967).

[40] N. Arkani-Hamed, A. G. Cohen and H. Georgi, Phys. Rev. Lett. **86**, 4757 (2001) [arXiv:hep-th/0104005].

[41] M. Harada, M. Tanabashi and K. Yamawaki, Phys. Lett. B **568**, 103 (2003) [arXiv:hep-ph/0303193].

[42] D. T. Son and M. A. Stephanov, Phys. Rev. D **69**, 065020 (2004) [arXiv:hep-ph/0304182].

[43] M. Piai, A. Pierce and J. Wacker, arXiv:hep-ph/0405242.

[44] R. S. Chivukula, M. Kurachi and M. Tanabashi, JHEP **0406**, 004 (2004) [arXiv:hep-ph/0403112].

[45] F. J. Gilman and H. Harari, Phys. Rev. **165**, 1803 (1968).

[46] S. Weinberg, Phys. Rev. **177**, 2604 (1969).

[47] J. J. Sakurai, *Currents and Mesons*, University of Chicago Press, Chicago (1969).

[48] T. Banks and A. Zaks, Nucl. Phys. B **196**, 189 (1982); Y. Iwasaki, K. Kanaya, S. Sakai and T. Yoshie, Phys. Rev. Lett. **69**, 21 (1992); Y. Iwasaki, K. Kanaya, S. Kaya, S. Sakai and T. Yoshie, Prog. Theor. Phys. Suppl. **131**, 415 (1998) [hep-lat/9804005]; R. Oehme and W. Zimmermann, Phys. Rev. D **21**, 471 (1980); R. Oehme and W. Zimmermann, Phys. Rev. D **21**, 1661 (1980);

M. Velkovsky and E. V. Shuryak, Phys. Lett. B **437**, 398 (1998) [hep-ph/9703345]; V. A. Miransky and K. Yamawaki, Phys. Rev. D **55**, 5051 (1997) [Erratum-ibid. D **56**, 3768 (1997)]. [hep-th/9611142].

[49] T. Appelquist, J. Terning and L. C. R. Wijewardhana, Phys. Rev. Lett. **77**, 1214 (1996) [arXiv:hep-ph/9602385]. T. Appelquist, A. Ratnaweera, J. Terning and L. C. Wijewardhana, Phys. Rev. D **58**, 105017 (1998) [arXiv:hep-ph/9806472].

[50] M. Harada, M. Kurachi and K. Yamawaki, Phys. Rev. D **68**, 076001 (2003) [arXiv:hep-ph/0305018].

[51] B. Holdom, Phys. Lett. B **150**, 301 (1985); K. Yamawaki, M. Bando and K. i. Matumoto, Phys. Rev. Lett. **56**, 1335 (1986); T. Akiba and T. Yanagida, Phys. Lett. B **169**, 432 (1986); T. W. Appelquist, D. Karabali and L. C. R. Wijewardhana, Problem In Phys. Rev. Lett. **57**, 957 (1986); M. Bando, T. Morozumi, H. So and K. Yamawaki, Phys. Rev. Lett. **59**, 389 (1987).

[52] K. Yamawaki, Phys. Lett. B **118**, 145 (1982).

[53] See, e.g., the proceedings of the conferences: S. Ishida et al “Possible existence of the sigma meson and its implication to hadron physics”, KEK Proceedings 2000-4, Soryyushiron Kenkyu 102, No. 5, 2001; D. Amelin and A. M. Zaitsev, “Hadron spectroscopy: ninth international conference on hadron spectroscopy HADRON 2001, AIP conference proceedings No. 619; A. H. Fariborz, “Scalar mesons: an interesting puzzle for QCD”, SUNY Institute of Technology, Utica, NY, 16-18 May 2003, AIP conference proceedings No. 688.

[54] M. Harada, F. Sannino and J. Schechter, Phys. Rev. D **54**, 1991 (1996) [arxiv:hep-ph/9511335].

[55] R. L. Jaffe, Phys. Rev. D **15**, 267 (1977); Phys. Rev. D **15**, 281 (1977).

[56] D. Black, A. H. Fariborz, F. Sannino and J. Schechter, Phys. Rev. D **59**, 074026 (1999) [arxiv:hep-ph/9808415].

[57] Y. Hidaka, O. Morimatsu and M. Ohtani, arXiv:hep-ph/0512375.

[58] U. G. Meissner, Phys. Rept. **161**, 213 (1988).